Constraining dark energy

V.Ruhlmann-Kleider
CEA/Irfu/DPhP - Saclay

1) State of the art, Type Ia supernovae (SNe Ia)
2) Baryonic acoustic oscillations (BAO) and beyond (RSD)
3) **Weak lensing (WL)**
4) The H_0 tension

Weak lensing

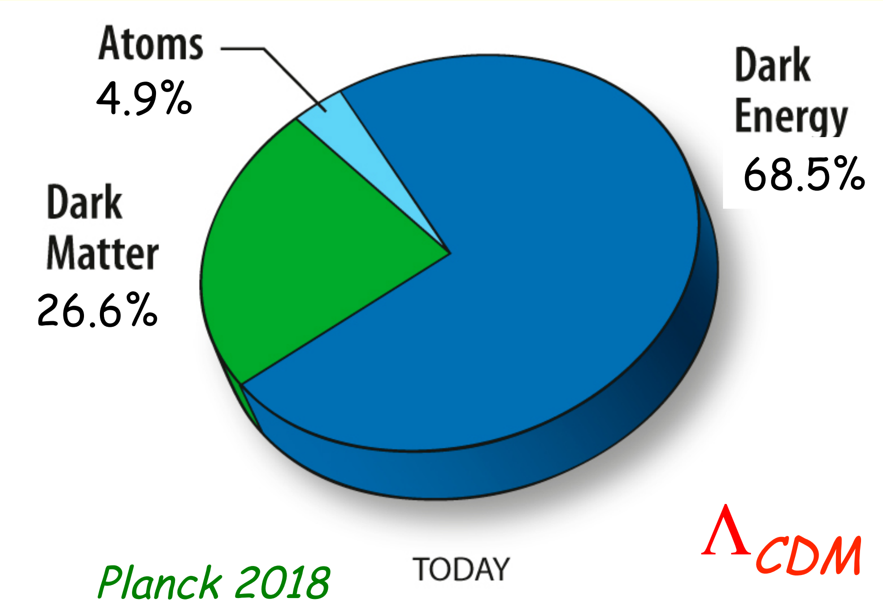

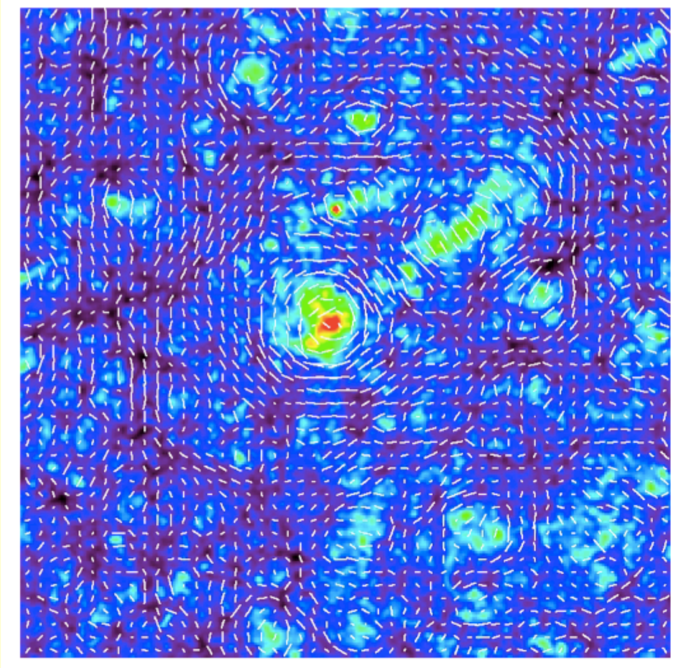

Credit: T.Hamana

1. Weak gravitational lensing, a brief introduction
2. Results
3. Prospects: Euclid, LSST, WFIRST

Method

Weak gravitational lensing

- Gravitational lensing: bending of light by mass along the line of sight to an observed source
  ⇒ distorted image of the source

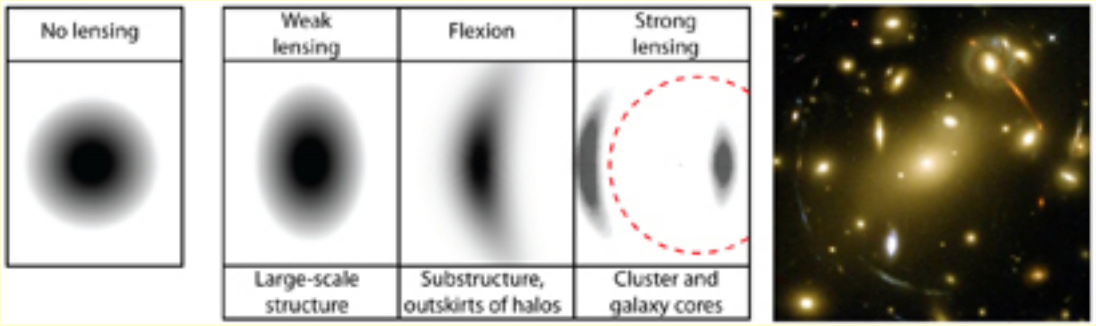

strong & weak lensing due to cluster Abell 2218

- Weak lensing ≡ gravitational lensing by large scale structures
  ⇒ distorted (= sheared) images of distant galaxies
  ⇒ 3D distribution of total matter (dark + luminous)
  ⇒ probe of geometry and structure

Shear and convergence

- Image distortion modelling: mapping between source (S) and image (I) planes:

$$\delta \boldsymbol{x}_i^S = \boldsymbol{A}_{ij} \delta \boldsymbol{x}_j^I \qquad \delta\vec{\boldsymbol{x}} \equiv \text{separation vector}$$

with:

$$\boldsymbol{A} = \begin{pmatrix} 1-\kappa-\gamma_1 & -\gamma_2 \\ -\gamma_2 & 1-\kappa+\gamma_1 \end{pmatrix} \qquad \text{distortion matrix}$$

- κ : convergence → isotropic magnification
- (γ_1, γ_2) : two-component shear → anisotropic stretch
- $|\gamma| = \sqrt{\gamma_1^2 + \gamma_2^2}$: total shear weak lensing limit: $\boxed{\kappa, |\gamma| \ll 1}$
- source magnification : $\mu = \dfrac{1}{|1-\kappa|^2 - |\gamma|^2} \underset{WL}{\approx} 1 + 2\kappa + O(\kappa^2, \gamma^2)$

Cosmic shear field

- $\kappa,|\gamma|\leq O(\textit{few}\ \%)$ ⇒ images weakly lensed ⇒statistical measurement on a large number (at least a few hundreds) of distant galaxies
- Cosmic shear ≡ statistical signal due to weak lensing

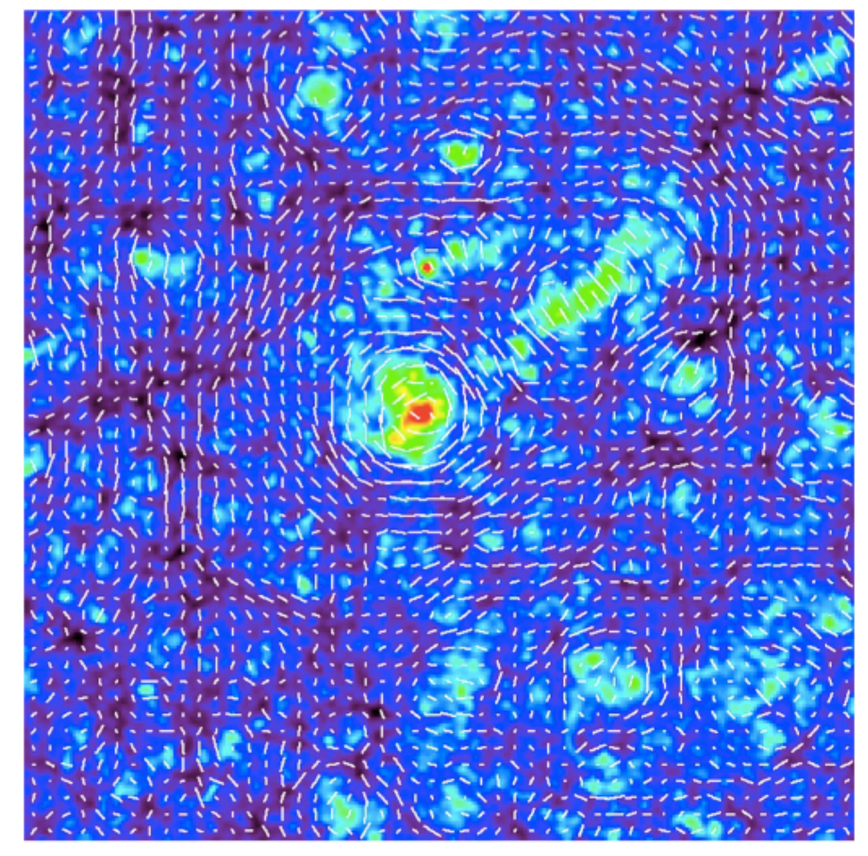

cosmic shear field (white) compared with mass distribution (over/underdense regions = bright/dark) (N-body simulation)

- Principal statistics: angular power spectrum & 2-point correlation function

Credit: T.Hamana

Shear/convergence angular power spectrum

- For source galaxies at z_s:

$$P_\kappa^\ell(z_s) = \int_0^{z_s} \frac{dz}{H(z)D_A^2(z)} W(z)^2 \boxed{P_m(k=\ell/D_A(z), z)}$$

$P_m(k,z)$: matter power spectrum
$W(z)$: efficiency for lensing galaxies

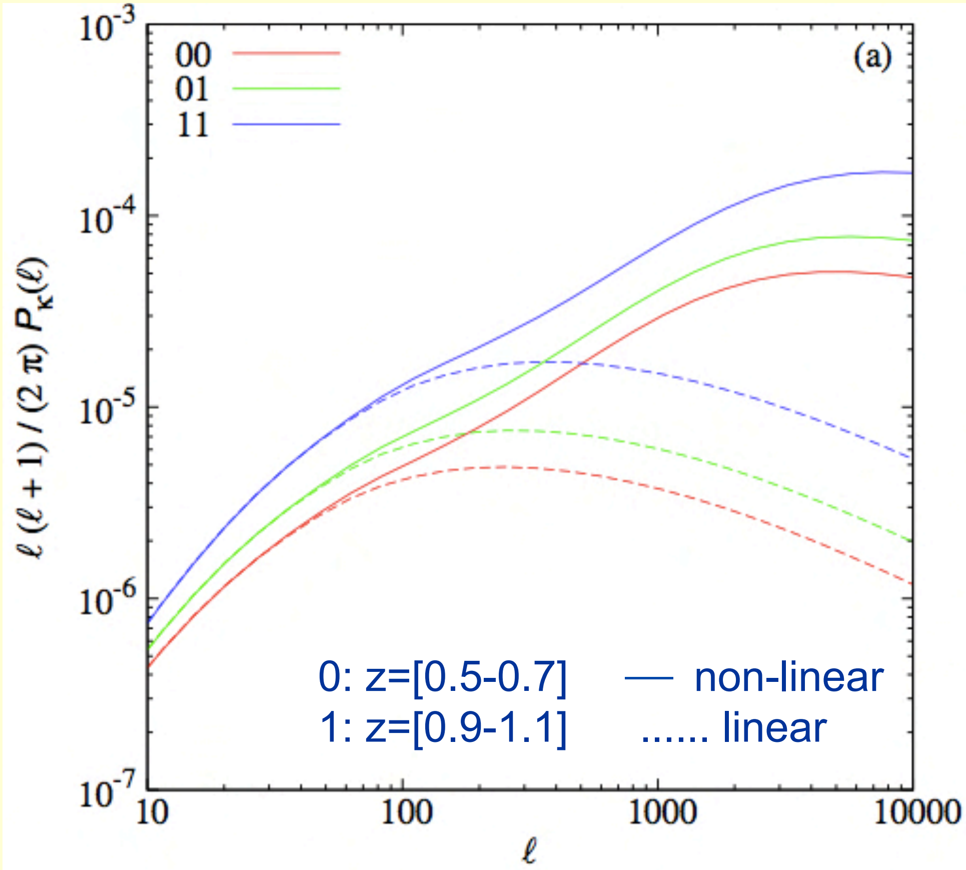

- WL probes both geometry and growth of structure
- WL radially projects density fluctuations

- more from : shear correlations between objects in different redshift bins (WL tomography)

  → f(z), w(z)

M.Kilbinger, 2015, Rep. Prog. Phys, 78, 086901

Sensitivity to cosmology parameters

- Projection along l.o.s : many features smeared out (e.g. BAO) ⇒loss of sensitivity

- P_κ^l most sensitive to:

$$\boxed{\sigma_8 \Omega_m^\alpha, \ \alpha \underset{lin}{\approx} 0.2\text{–}0.7}$$

σ_8 matter power spectrum normalization today

$\alpha \approx 0.25$ CMB, 0.5 at low z

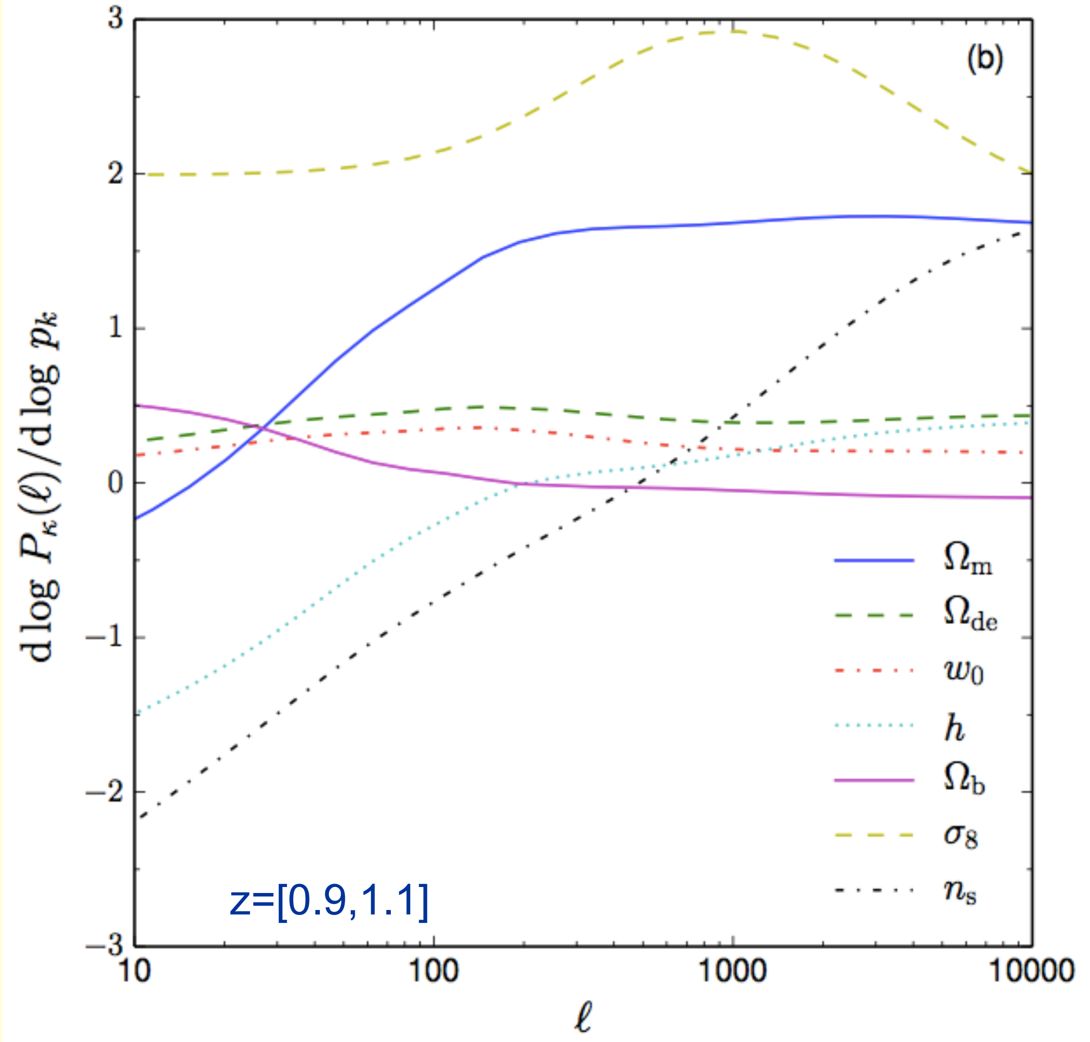

Shear correlation function

- Galaxy shape measurements ⇒galaxy ellipticities ⇒2PCF

- 2 component shear
  ⇒ 2 component CF

$$\xi_+(\vartheta) = \langle\gamma_t\gamma_t\rangle(\vartheta) + \langle\gamma_\times\gamma_\times\rangle(\vartheta)$$
$$\xi_-(\vartheta) = \langle\gamma_t\gamma_t\rangle(\vartheta) - \langle\gamma_\times\gamma_\times\rangle(\vartheta)$$

ϑ : angular separation

NB: $\xi_+(\vartheta) = 2PCF(\kappa)$

NB: several derived 2nd order statistics exist

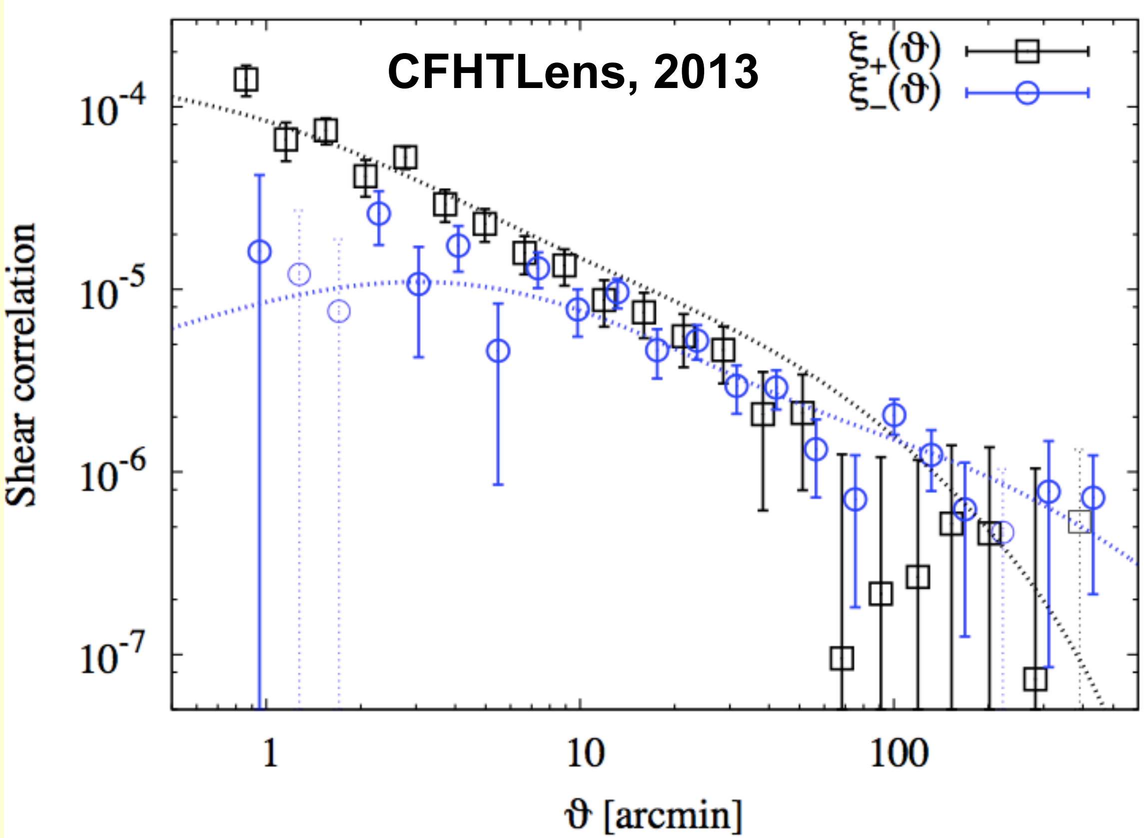

M.Kilbinger, 2015, Rep. Prog. Phys, 78, 086901

Requirements for precise measurements

- Statistical uncertainty at large scale:

shot noise

$$\Delta P_\kappa^\ell = \sqrt{\frac{2}{(2l+1)f_{sky}}}\left[P_\kappa^\ell + \frac{\sigma^2(\gamma_i)}{n_{eff}}\right]$$

cosmic variance

  - f_{sky} survey area
  - σ_γ std dev in a single component shear (~ 0.2 typical)
  - n_{eff} effective number density of galaxies with well measured shapes

  ⇒ wide & deep survey, galaxy shape measurements with modest precision on individual galaxies but unbiased for the galaxy sample (currently 1% accuracy → 0.1%)

- Large samples means photometric redshifts for source galaxies

Systematics

- Observational systematics for shape measurements: PSF varies with atmospheric blurring, telescope distortions, CCD non-flatness and misalignment on the focal plane, pixelation…
  ⇒ bias calibration with a large and representative sample of observed and simulated galaxie, hence deep observations & image simulations

- Limited precision of photometric redshifts: bias < 0.1%, resolution $\sigma_z/(1+z) \approx 3\%$, outlier rate < 10% (<1% tomography)
  ⇒ large spectroscopic sample for calibration ($10^4 \rightarrow 10^5$)

- Interpretation: predictions deeply in the non-linear regime (⇒N-body simulations) + non-Gaussian errors at small scale

- Modelling of intrinsic alignment of galaxy shapes (on their surrounding grav. potentials) ⇒astrophysics input

Results

Precursors, 2000-2013

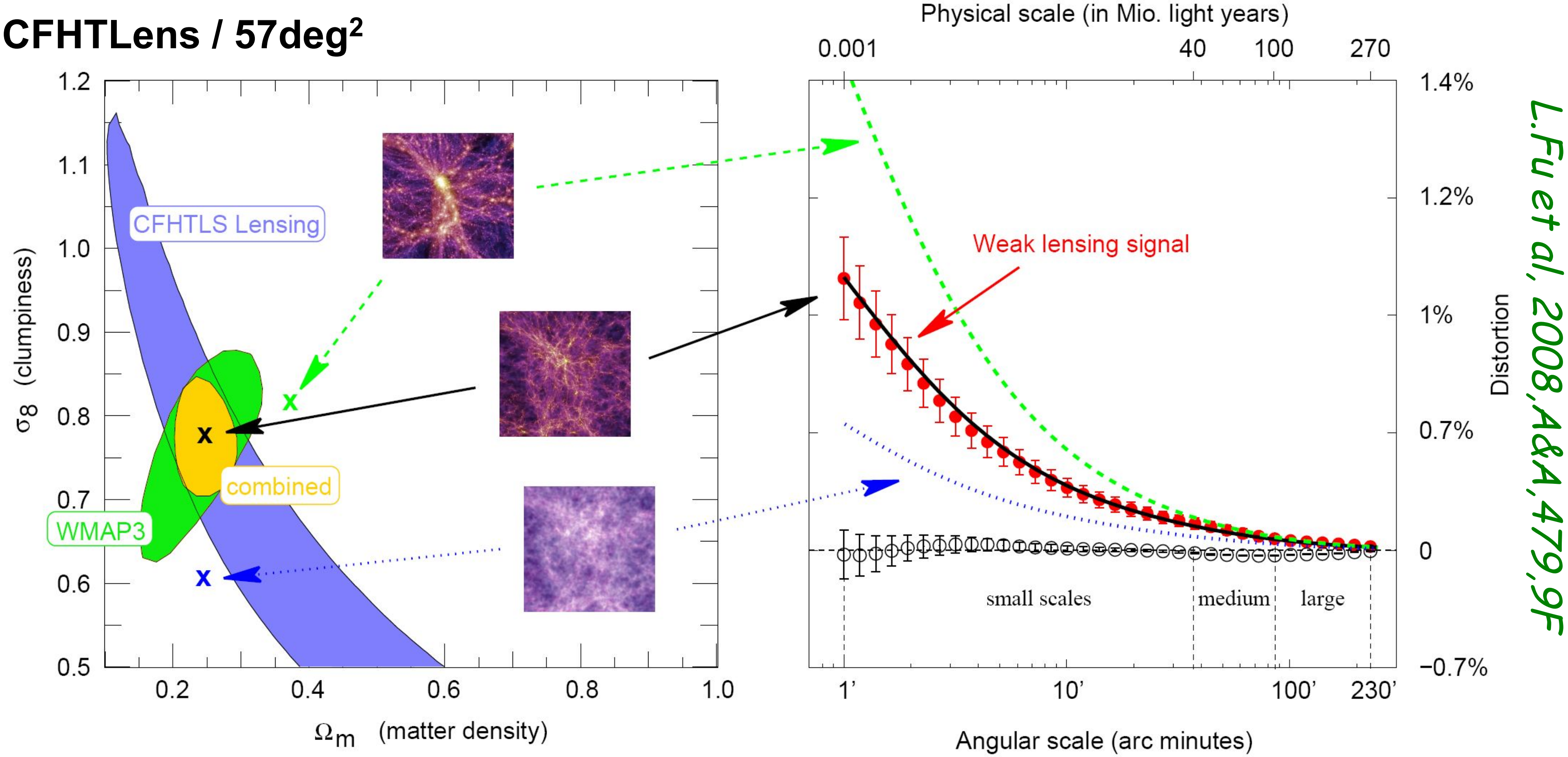

- CFHTLens (2003/2008), 170deg^2, ugriz, 5σ depth ≈ 25.5 i_{AB}, 17 gal. arcmin^{-2} + photo-z's from CFHTLS deep fields: $\sigma_z/(1+z)$~4% & outlier rate~4% in $0.2<z<1.3$ →$n(z_s)$ estimate

Ongoing surveys, since 2013

Project	deg^2	sources	N/$arcmin^2$	r lim	z_s	filters	aim deg^2
DES-Y1 (2013, 5yrs)	1,321	26 10^6	5.14	23.2 (10σ)	0.2/1.3	grizY	5,000
HSC-Y1 (2014, 6yrs)	137	9 10^6	16.5	26 (5σ)	0.3/1.5	grizY	1,400
KV-450 (2015)	450	12 10^6	6.85	25.2 (5σ)	0.1/1.2	ugri+NIR	1,300

- DES-Y1: multi-probe survey : shear tomography (4 bins) + galaxy clustering and their cross-correlation (650,000 lenses)
  → combination of probes within the same survey
- HSC-Y1: shear tomography (4 bins) from the wide HSC survey
- KiDsViking-450: shear tomography survey (5 bins)
  → accurate photometric redshift calibration

T.M.C.Abbott et al, 2018, Phys. Rev. D98, 043526

DES-Y1

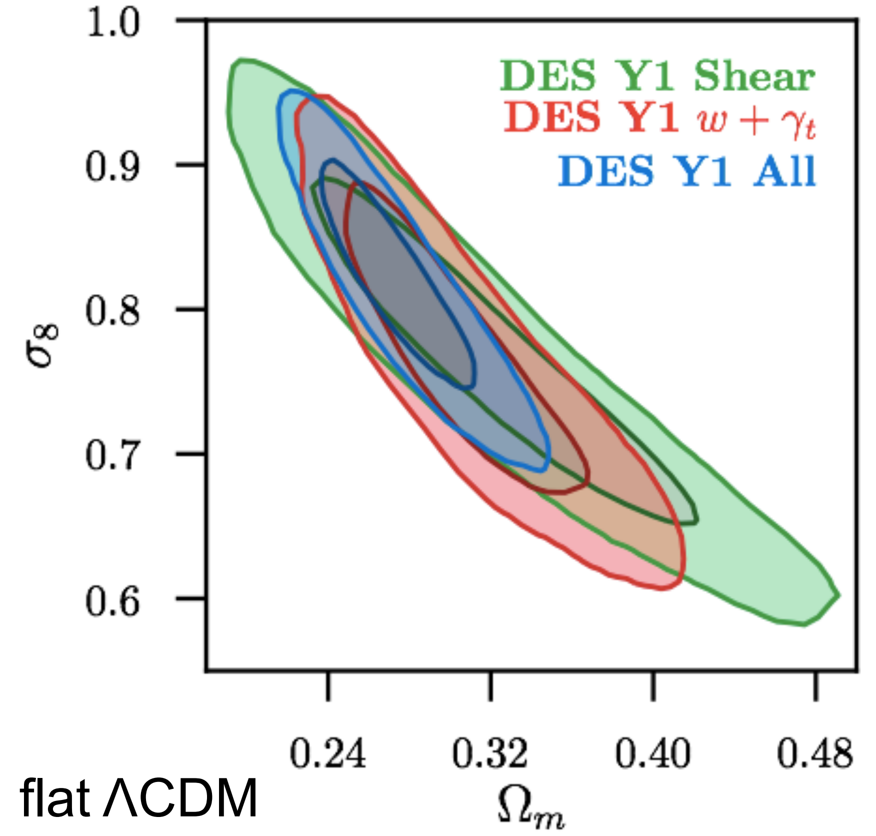

- Three probes combined:
  - $\xi_\pm(\vartheta)$ 2PCF of source galaxy ellipticities
  - $w(\vartheta)$ angular 2PCF of lens galaxies
  - $\gamma_t(\vartheta)$ tangential shear of sources x lens galaxy positions (so-called galaxy-galaxy lensing)

- Combination:
  - self-calibrates some WL systematics (e.g. intrinsic alignment, photometric redshift uncertainties…)
  - solves for galaxy bias

DES-Y1: one of the two shear measurements

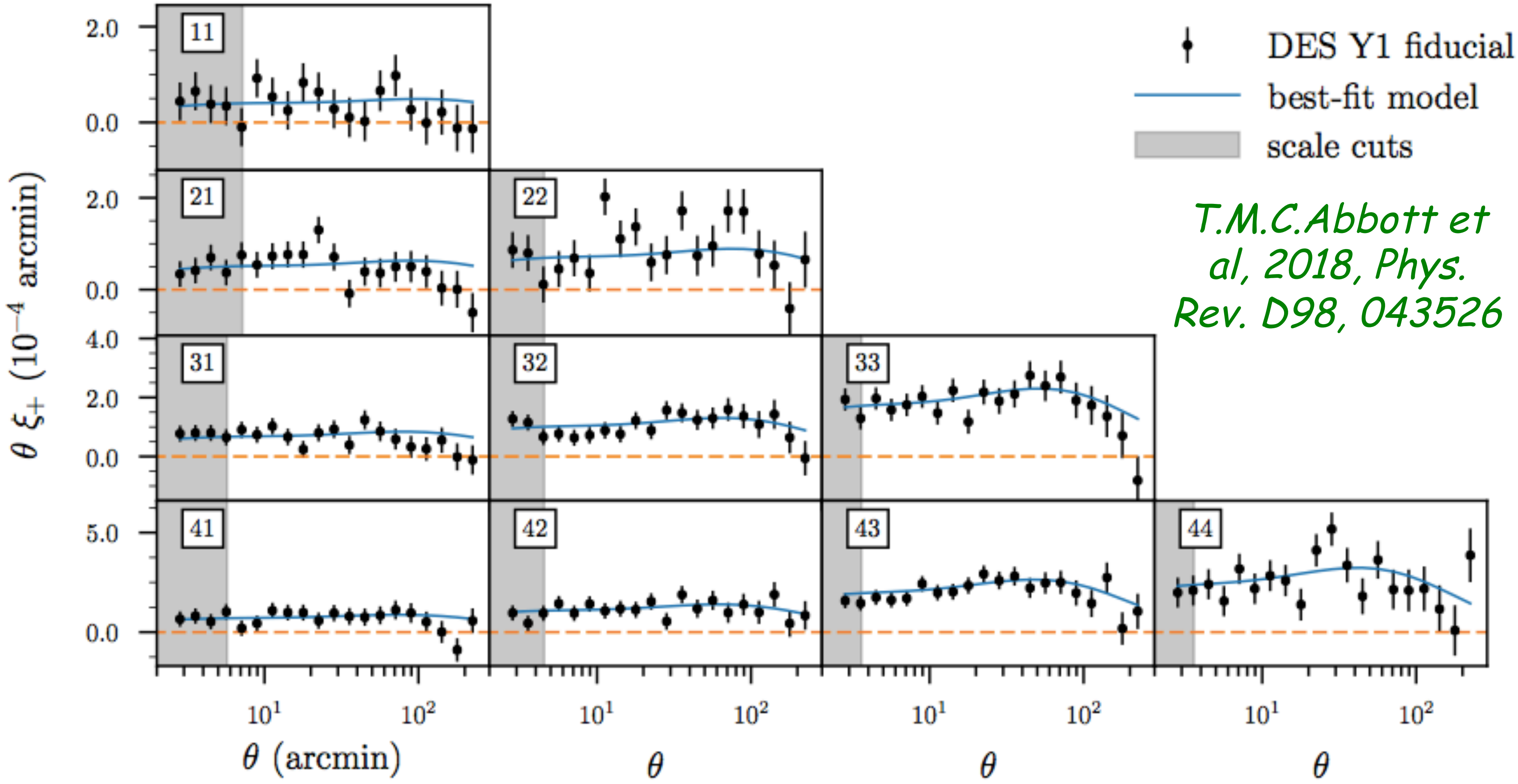

T.M.C.Abbott et al, 2018, Phys. Rev. D98, 043526

- Source sample distributed in 4 photo-z bins, low scales excluded (to reduce uncertainties in modelling intrinsic alignment and baryonic effects)

DES-Y1: clustering measurements

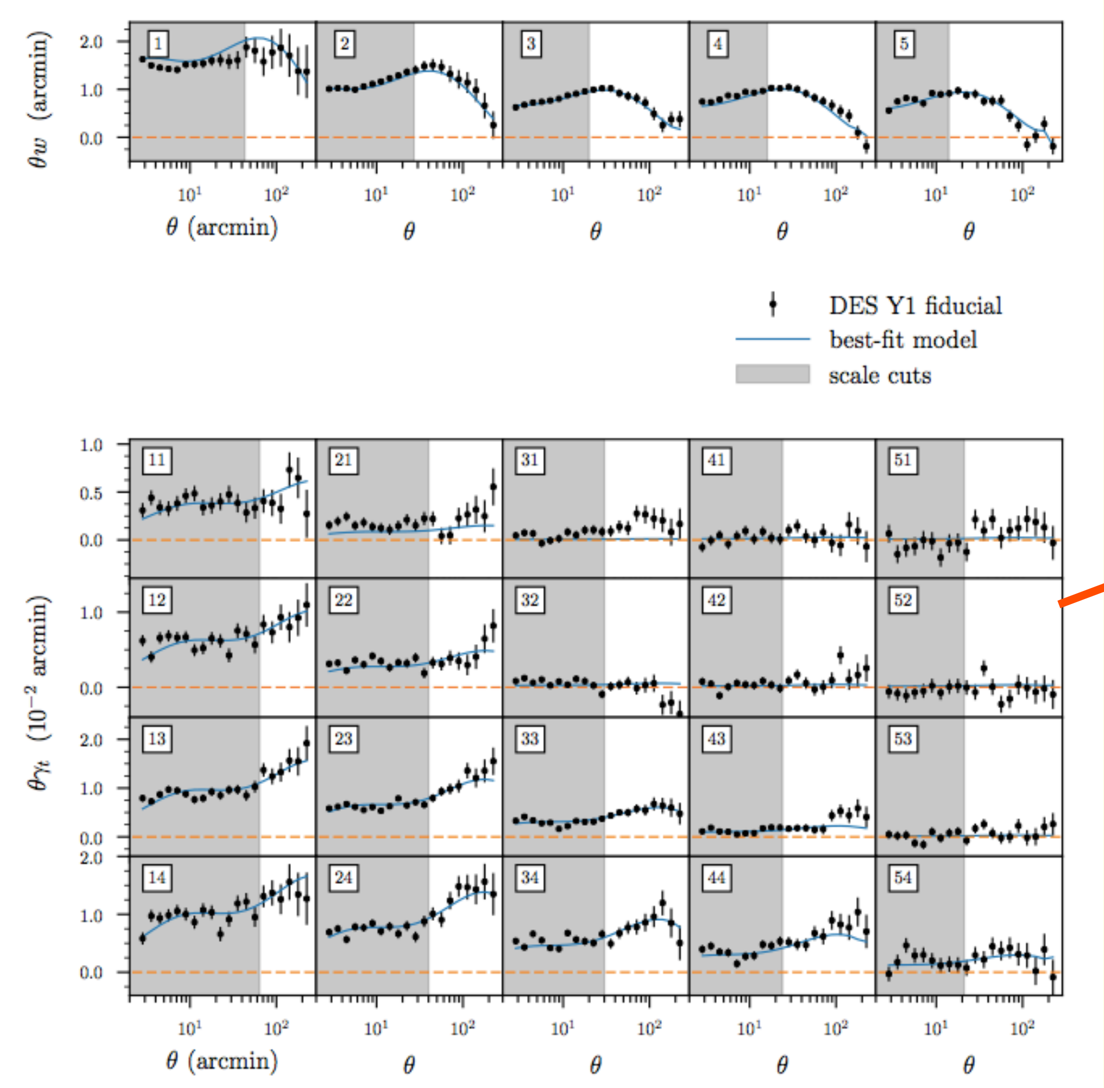

lens x lens

T.M.C.Abbott et al, 2018, Phys. Rev. D98, 043526

<u>Note</u>: when $z_l > z_s$ no signal expected

lens x shear

- Lens sample distributed in 5 photo-z bins, low scales excluded (because of modelling uncertainties in the non-linear regime)

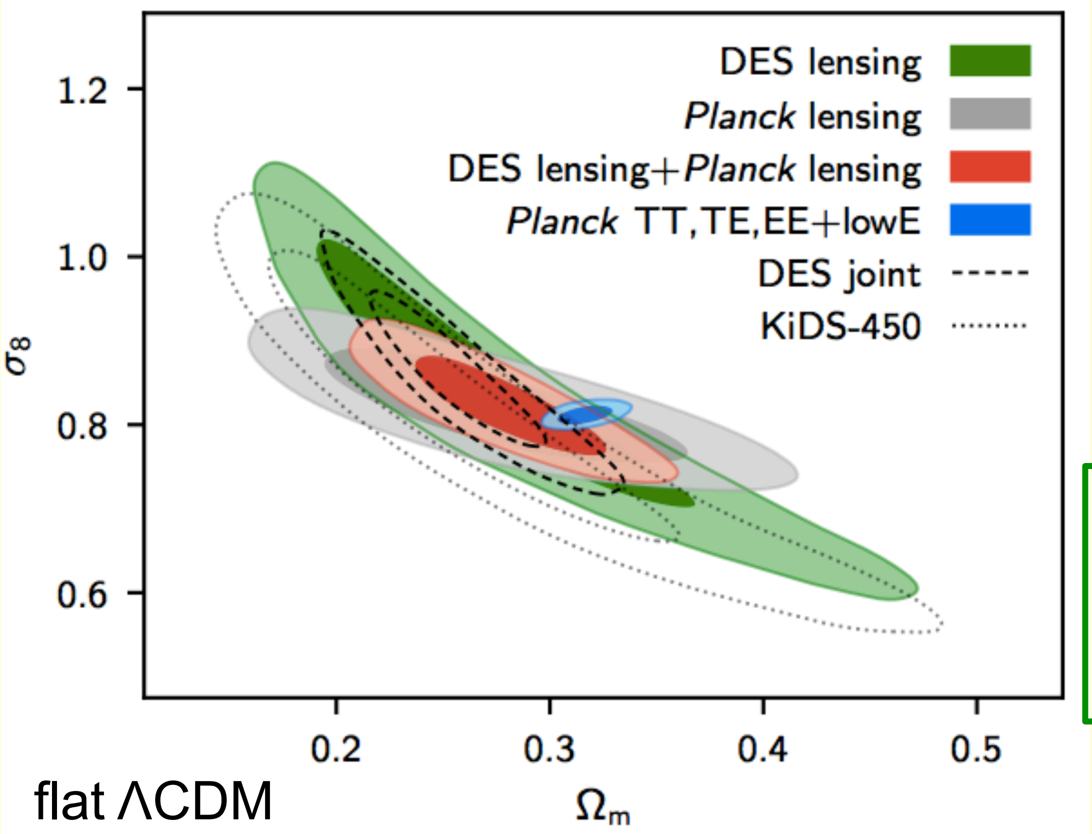

Comparison with CMB

Planck Collaboration, arXiv:1807.06209

	Planck all	*DES all*
S_8	0.832±0.013	0.792±0.024
Ω_m	0.315±0.007	$0.257^{+0.023}_{-0.031}$

with $S_8 \equiv \sigma_8 (\Omega_m / 0.3)^{0.5}$

- Lensing from DES (& other WL surveys) agree with CMB lensing.
- Mild tension (2σ) between lensing and Planck T&E constraints: can Λ_{CDM} reconcile measurements of high redshift (linear) perturbations and low redshift (non linear) clustering ?
- Same trend with cluster data. More (precise) data needed for a conclusive evidence.

KiDS-VIKING-450

H.Hildebrandt et al, arXiv:1812.06076

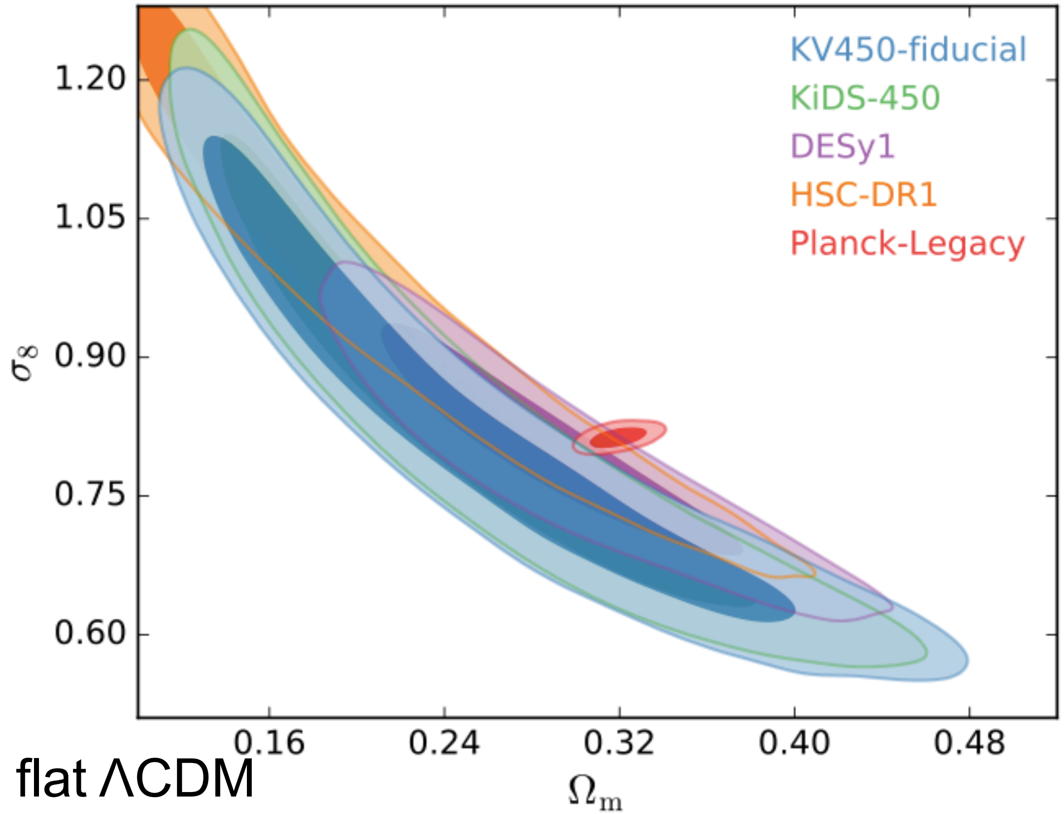

flat ΛCDM

- 9 band imaging (optical+NIR)

⇒ robust source photo-z calibration

⇒ no hint of residual systematics

- 2.3σ discrepancy with Planck-2018
- S_8 increase with calibration based on COSMOS-15 photo-z ctlg: artificial (outliers) ? Could impact DES & HSC

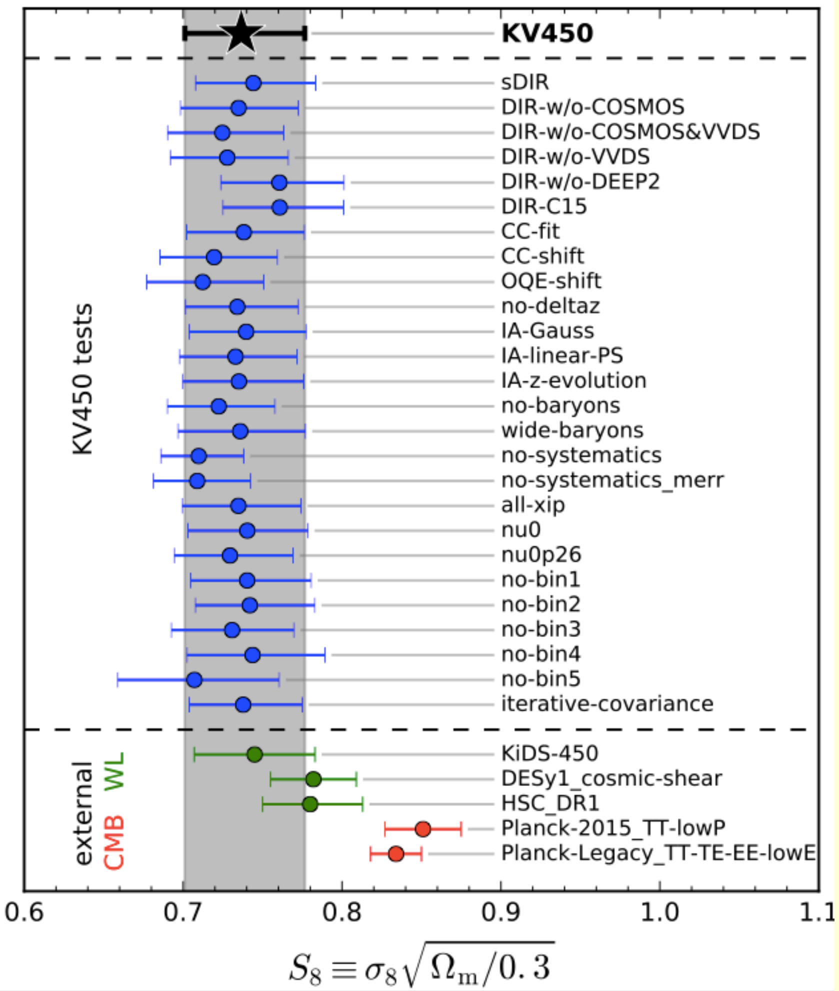

WL Summary

- weak lensing probes total matter distribution (so no need for a bias model) ⇒constrains geometry & growth rate
- tiny signal means tight constraints on survey design & analysis to control systematics (PSF control, unbiased photometric redshifts, non-linear predictions, mitigation of residual systematic effects....)

  systematics in shear measurements & photo-z bias must be < 1%
- many observables & statistics (shear & convergence, 2-pt statistics and derived functions, tomography, shear peak counts, higher order stat. ....)
- combination with clustering and galaxy-galaxy lensing : very helpful to constrain part of WL systematics (self-calibration)
- current status:
  - uncertainty on S_8 : stat ≳ syst
  - mild (2σ) tension between WL and CMB data (without lensing)
  - WL does not add much yet to current dark energy constraints

Prospects

Euclid

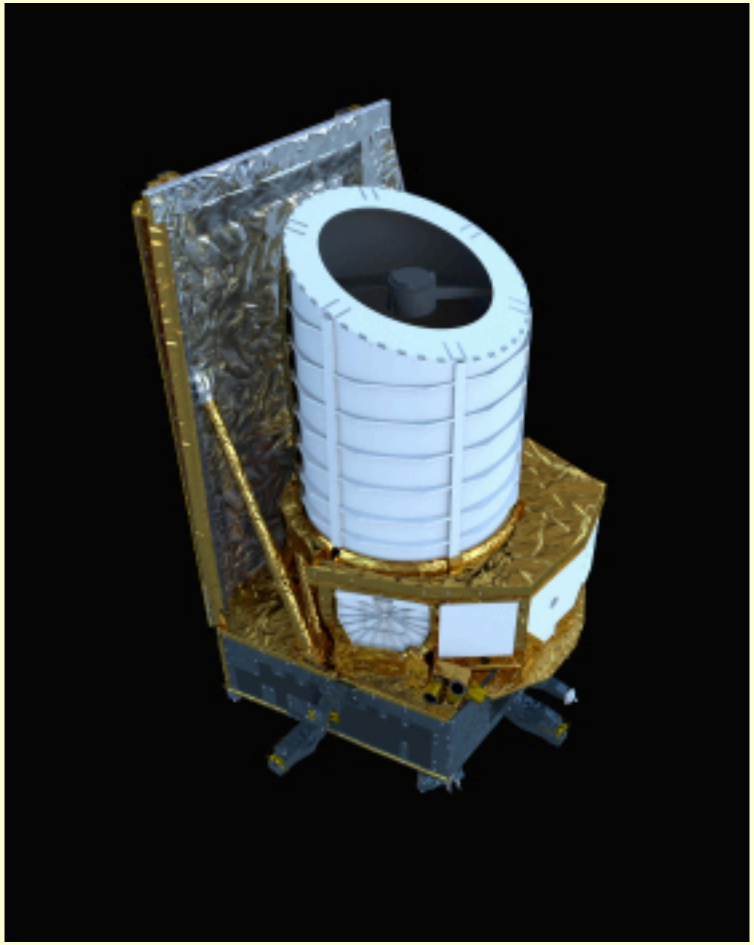

- 1.2 m mirror
- ~0.53 deg^2 FoV
- VIS: visual imager, 540 Megapixels
  - 0.55-0.9 μm, 1 broad R+I+Z band
- NISP: NIR photometry
  - 0.92-2.0 μm YJH bands

  and slitless spectroscopy
  - 0.92-1.85 μm (R=380)

- satellite, L2
- Launch 2022, 6yrs
- 15,000 deg^2, a billion galaxies

Euclid: an instrument/survey optimised for WL and BAO/RSD

(with additional (u)griz data from the ground : PanSTARRS, DES, KiDs.....)

Weak lensing and BAO/RSD with Euclid

- Euclid WIDE survey: 15,000 deg^2 (baseline, goal 20,000 deg^2)
- WL: imaging survey
  - a billion shape measurements up to $z=2$: VIS photometry (10σ extended source) depth $RIZ_{AB} \approx 24.5$, source density 30 $arcmin^{-2}$
  - source galaxy photo-z's: $\sigma_z/(1+z) \lesssim 5\%$, <10% outliers, bias<2 10^{-3} NISP photometry: (5σ point source) depth in Y, J, $H_{AB} \approx 24$ +griz photometry from the ground (DES, KiDs, Pan-STARRS, LSST…). photo-z calibration : 10^5 accurate spectroscopic redshifts required →NISP spectroscopy in deep fields + existing catalogs from the ground (SDSS, VVDS, zCOSMOS, DEEP2, VIPERS, VIMOS ….)
- BAO/RSD: spectroscopic survey (NISP spectroscopy), 50 million redshifts (Hα emission line galaxies), $0.7 < z < 2.1$.

- Euclid DEEP survey (2 mag deeper, 2x>10deg^2): slitless calibration spectroscopy for WL photo-z's (in $0.7<z<2.0$), stability monitoring, control of the wide survey radial selection function…

Euclid vs DESI forecast on clustering (RSD)

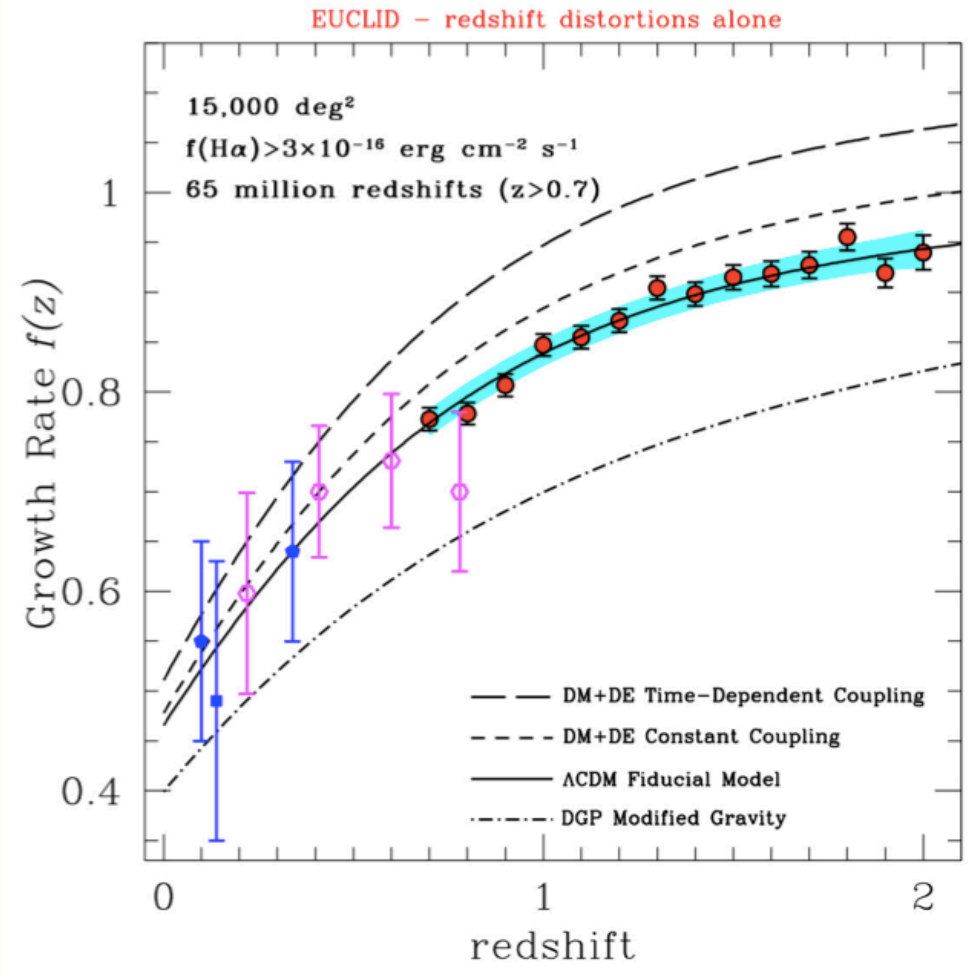

R.Laureijs et al, Euclid Definition Study Report, arXiv:1110.3193

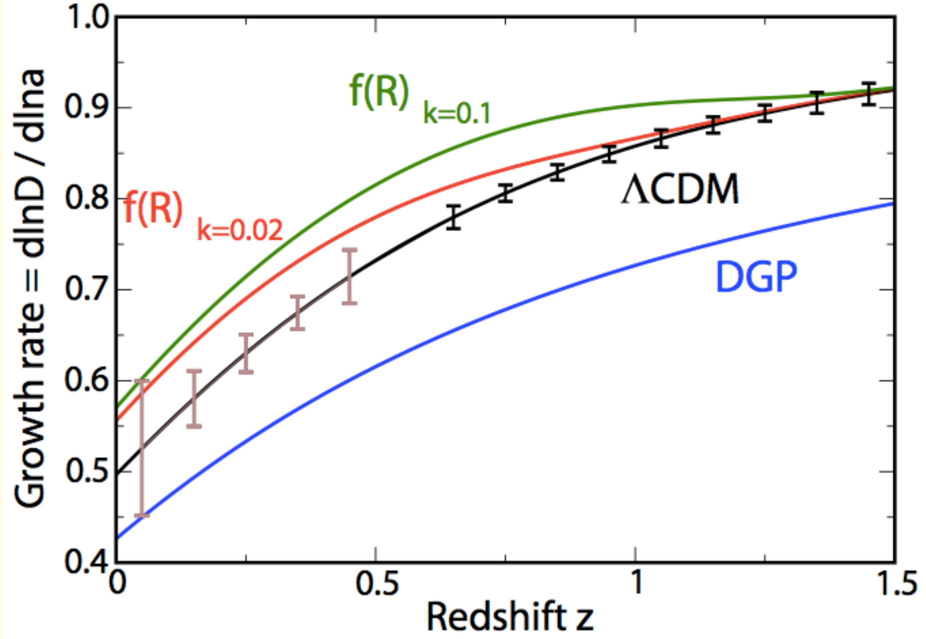

DESI prospects, arXiv:1611.00036

- similar precision
- extended redshift coverage
  (DESI z<0.7, Euclid z>1.5)

Euclid forecast on weak lensing

R.Laureijs et al, Euclid Definition Study Report, arXiv:1110.3193

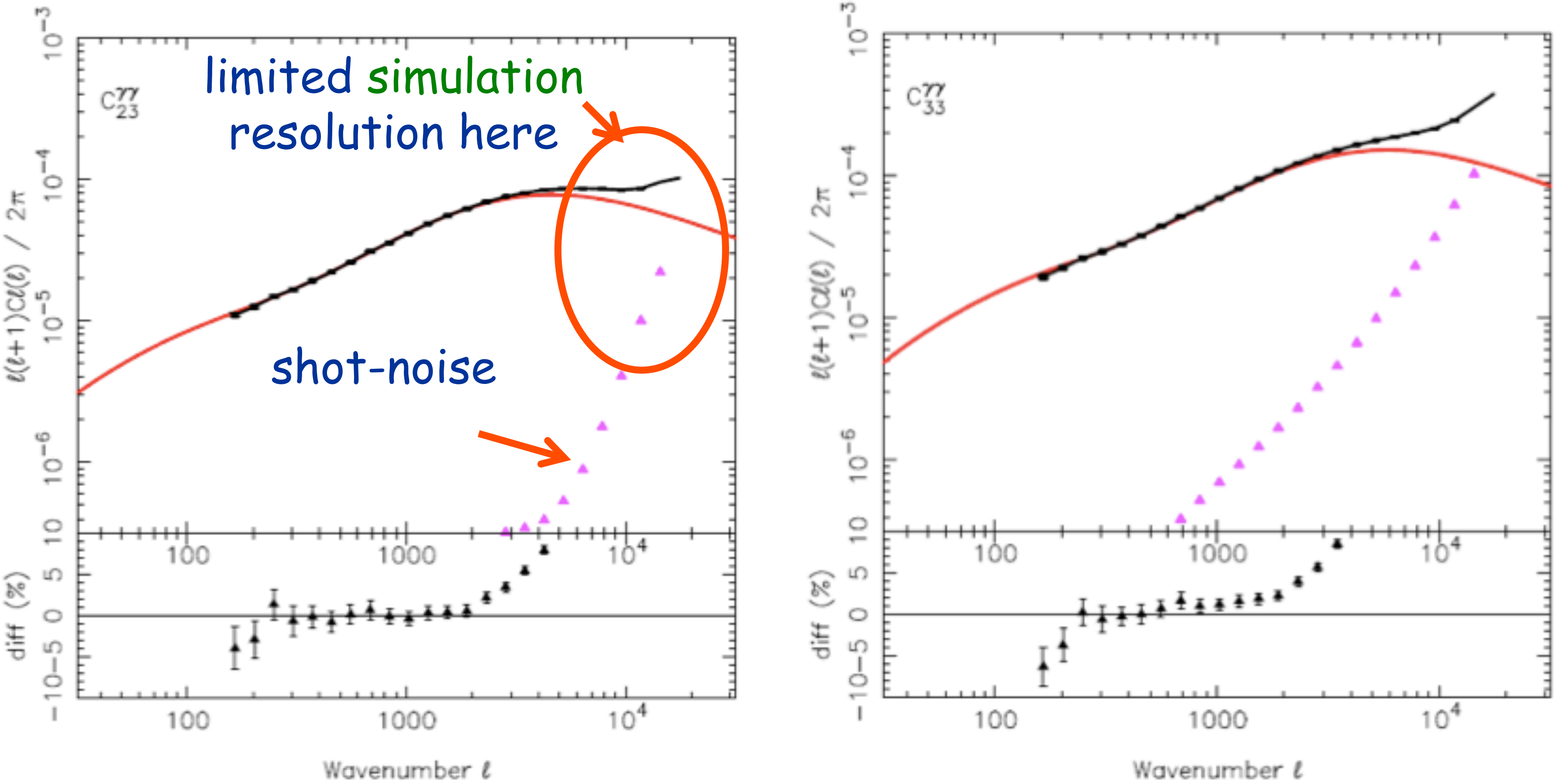

- expected shear spectrum recovered to better than 1% over all signal-dominated scales (l<<2,000), higher resolution simulation required to get realistic prospects at smaller scales.

Euclid forecast

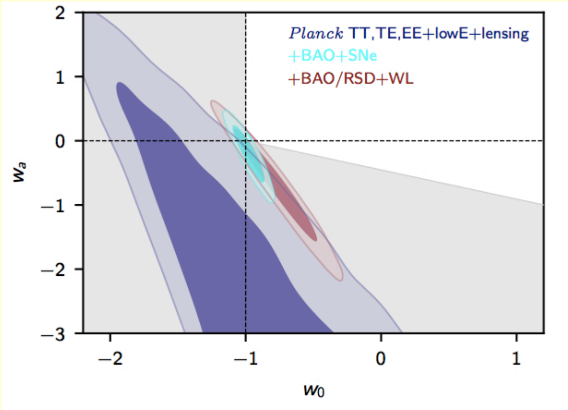

$\delta w = 0.032 = \delta w_p$

$\delta w_0 = 0.08 \quad \delta w_a \approx 0.3$

BAO/RSD+WL:

$\boxed{\delta w_p \approx 0.015 \quad \delta w_a \approx 0.15}$

all Euclid probes (BAO/RSD,WL,CL,ISW):

$\boxed{\delta w_p \approx 0.013 \quad \delta w_a \approx 0.05}$

combined with Planck T & P data:

$\boxed{\delta w_p \approx 0.007 \quad \delta w_a \approx 0.04}$

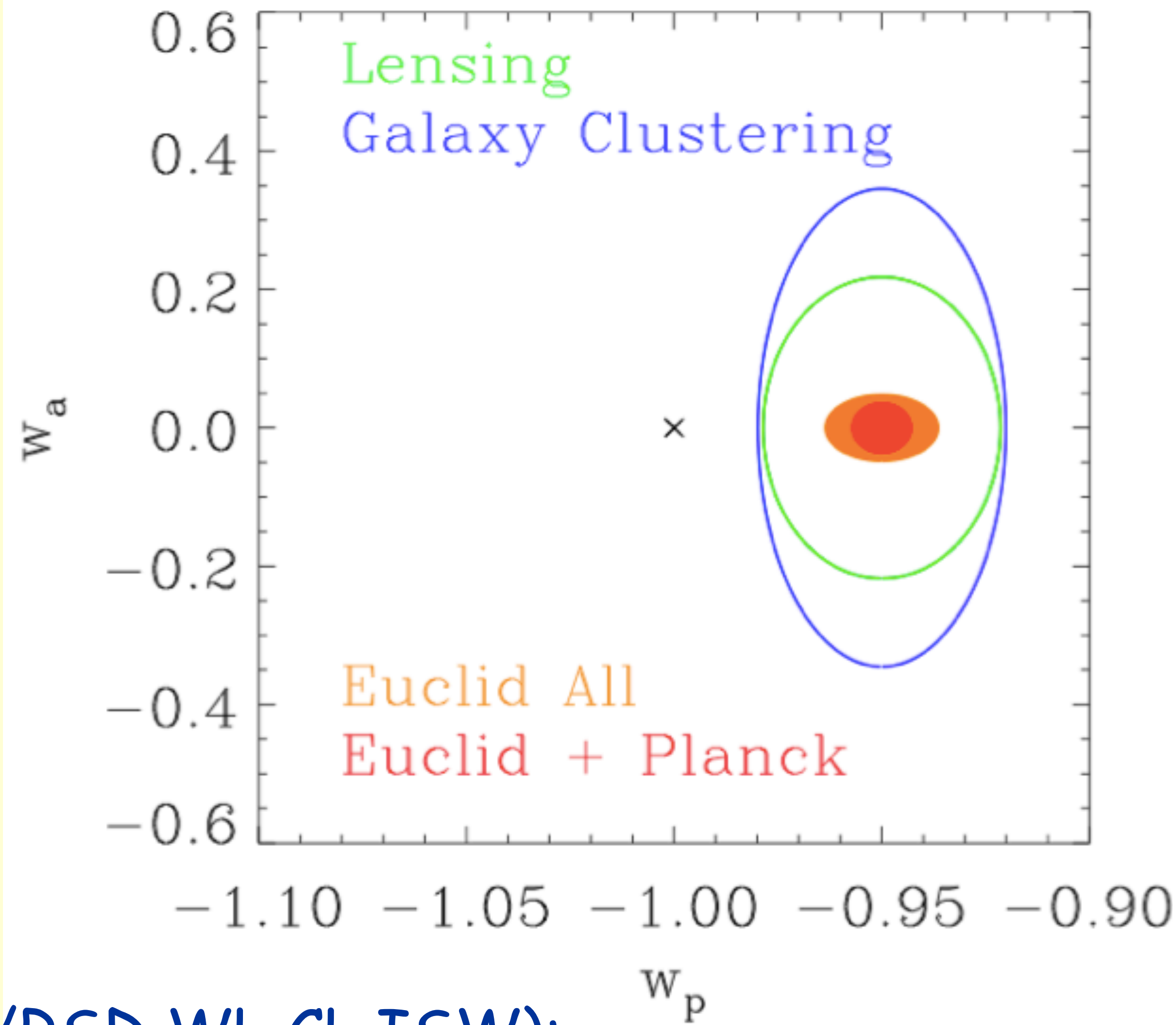

R.Laureijs et al, Euclid Definition Study Report, arXiv:1110.3193

Weak lensing with LSST

- LSST main survey:
  Wide-Fast-Deep survey

  - 18,000 deg^2
  - imaging 5σ point-source depth r_{AB}~ 27.5, source density 48 arcmin^{-2}
  - 2 billion galaxy shape measurements
  - photometric redshifts with $\sigma_z/(1+z)\sim 0.3\%$, bias$<10^{-3}(1+z)$

LSST Dark Energy Science Collaboration, arXiv:1809.01669

Z.Ivezic et al, arXiv:0805.2366v5 (May 2018)

depth

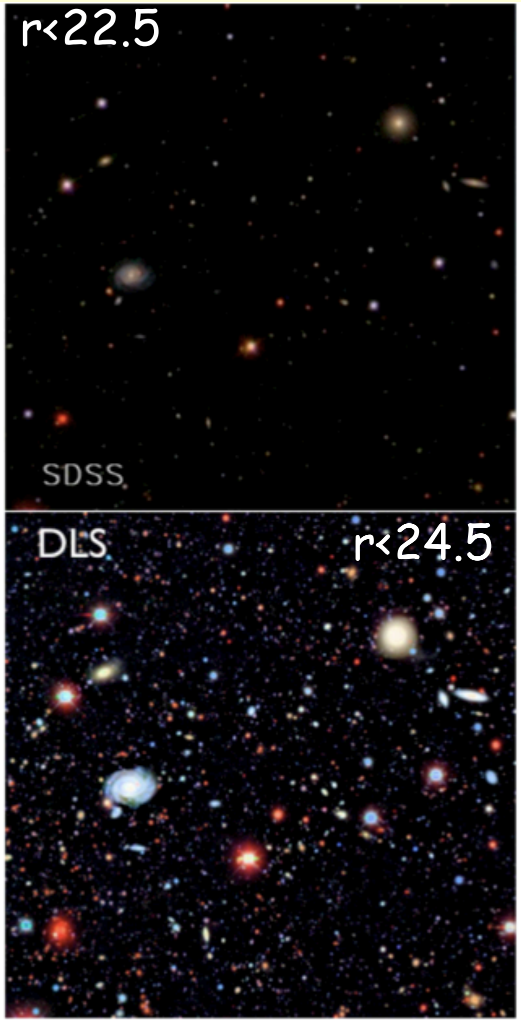

LSST will go 3mag deeper (after coadd)

angular resolution

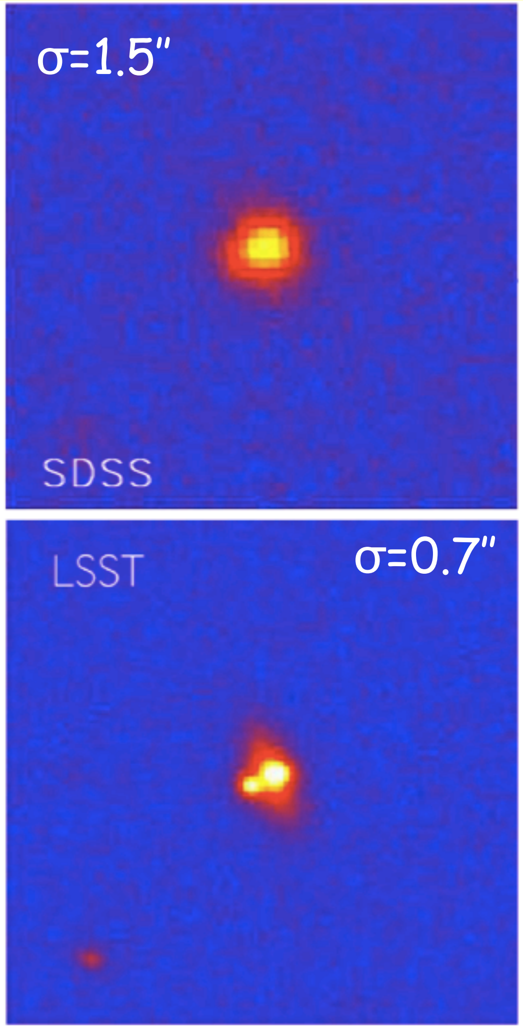

a lensed QSO (20x20 2″ images)

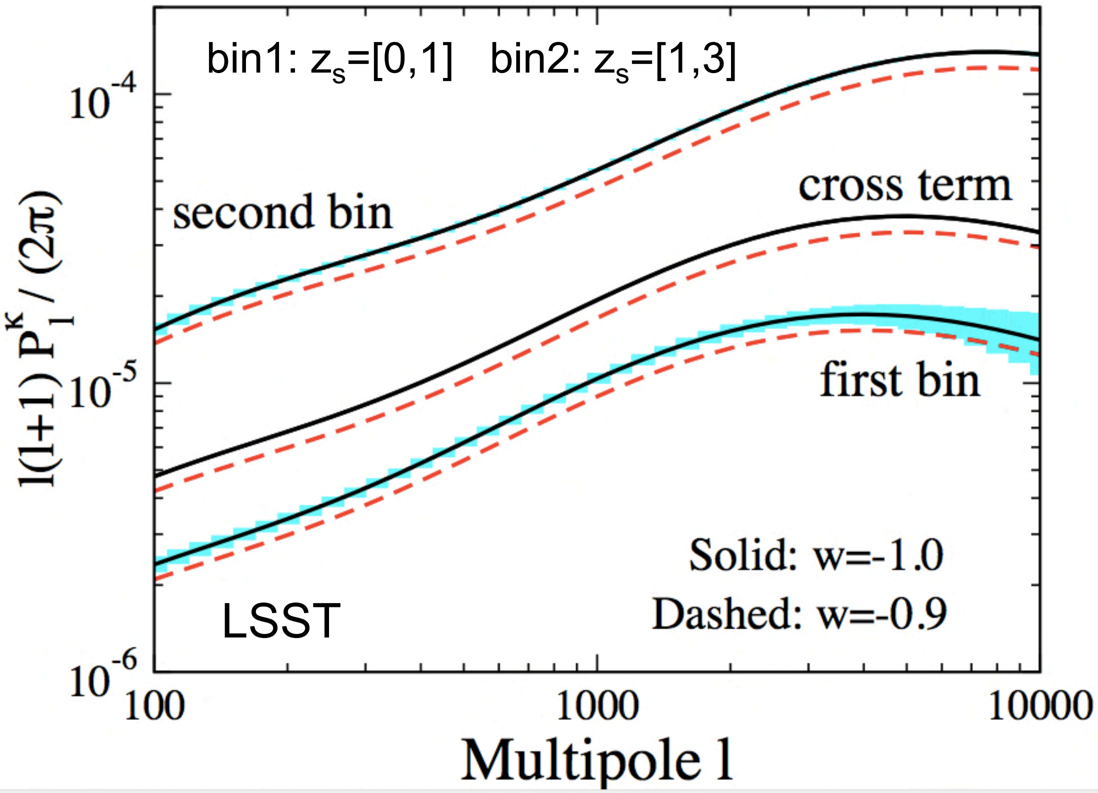

LSST vs Euclid forecast

(here: cosmic shear power angular spectrum)

*R.Laureijs et al, Euclid **Assesment Study** Report, arXiv:0912.0914*
(small scales: a bit optimistic at that time)

D.Huterer, D.L.Shafer, Rep. Prog. Phys. 81 (2018) 016901

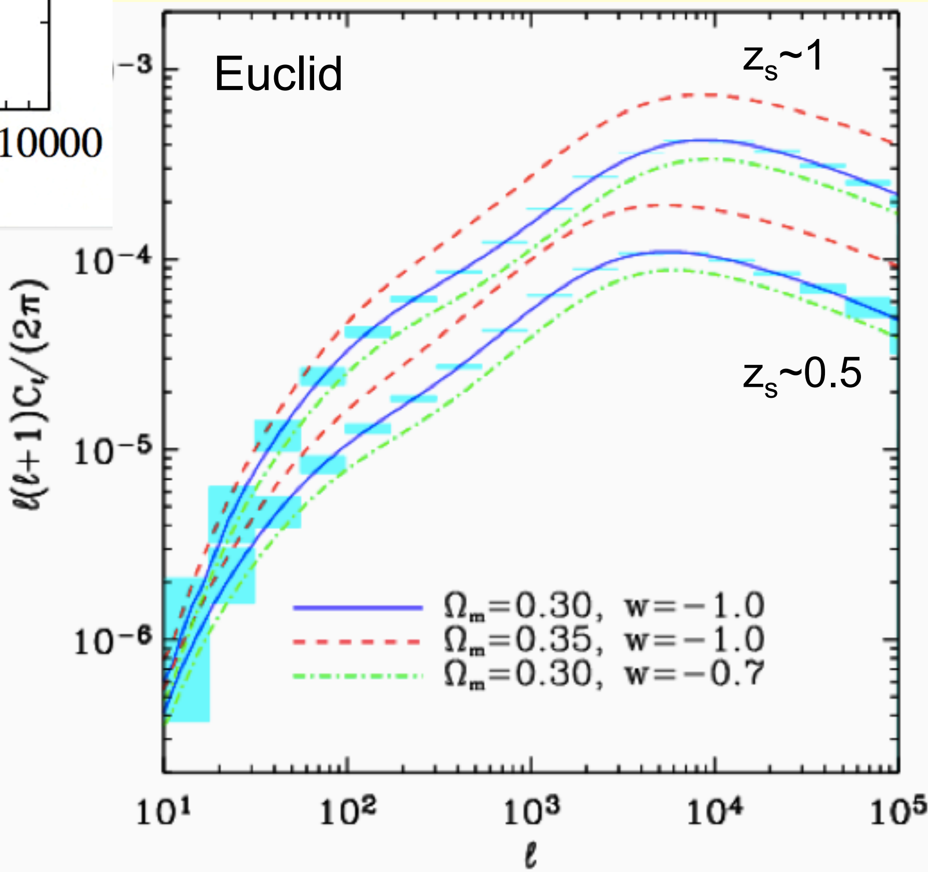

- similar performance on cosmic shear accuracy and sensitivity to cosmological parameters

LSST general forecast (cf. L1 & L2)

LSST Dark Energy Science Collaboration, arXiv:1809.01669

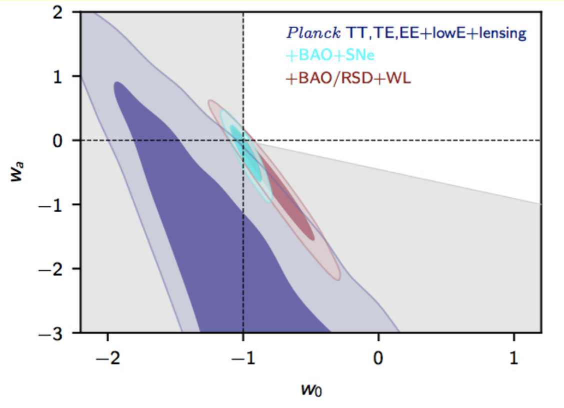

$\delta w=0.032=\delta w_p$

$\delta w_0=0.08 \quad \delta w_a\approx 0.3$

Clustering & WL combined
i.e.
joint analysis of shear-shear, galaxy-shear and galaxy-galaxy correlation functions (as in DES analysis, see slide 13).

all probes (cf L2):

$\delta w_0 \approx 0.025$
$\delta w_a \approx 0.15$

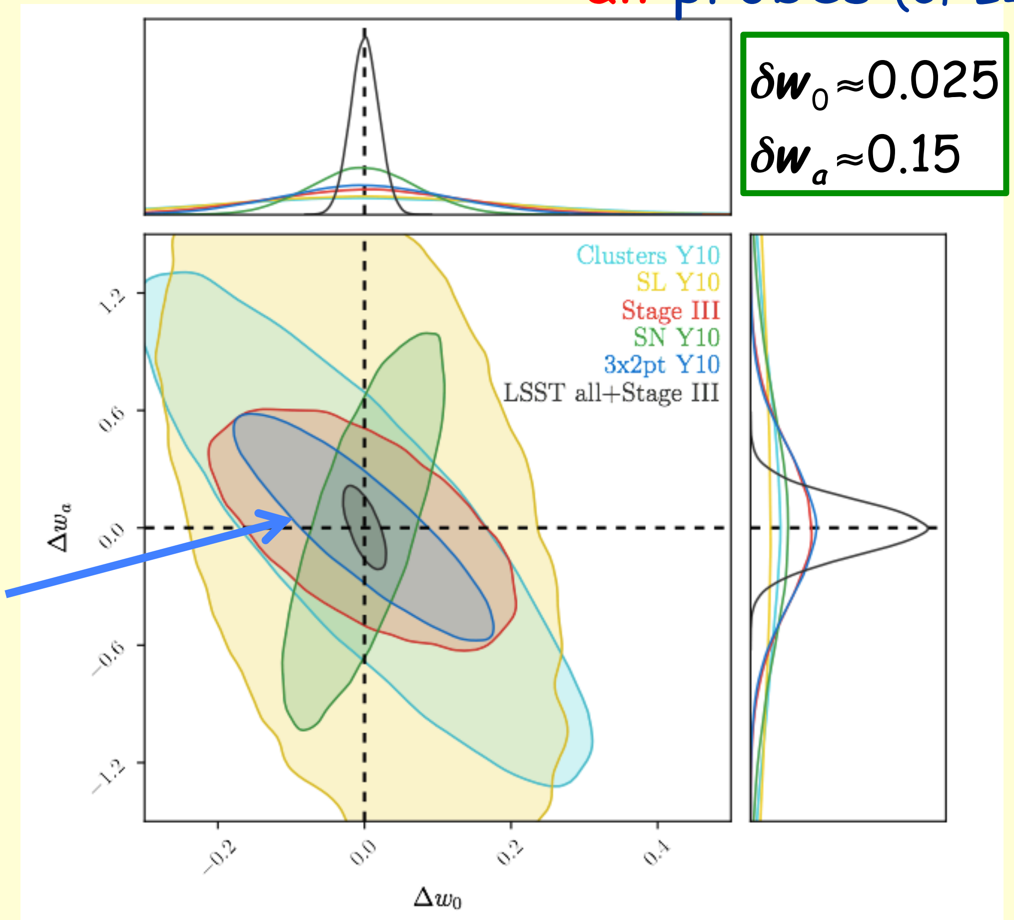

WFIRST forecast (see L2): same kind of joint analysis
Euclid forecast (slide 23): galaxy-shear NOT included in combination (yet)

Weak lensing with WFIRST

- WFIRST High Latitude imaging survey (2yrs spread over 5yrs): 2,000 deg^2, imaging & grism spectroscopy for photo-z calibration, (5σ point source) depth Y,J,H,$F_{AB} \lesssim 27$, source density in coadded images 50 arcmin^{-2}, 3.6 10^8 shape measurements, $\sigma_z/(1+z) \sim 4\%$

  Strong point: well-controlled systematics (high angular precision, photometric stability, low readout noise, coverage uniformity...)

z bins: δz=0.5

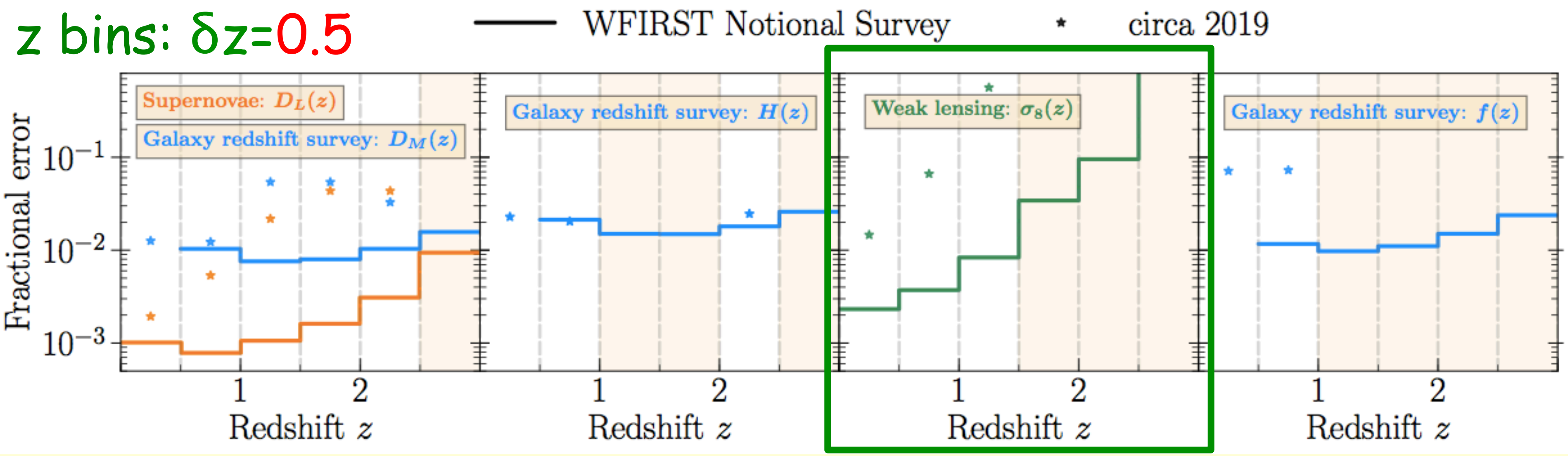

O. Doré et al, Astro2020 science white paper, arXiv:1904.011174

WFIRST forecast

all probes: $\delta w_p \approx 0.025 \quad \delta w_a \approx 0.13$ (cf L2)

WFIRST imaging only
(no BAO, no SN, photometric galaxy clustering in joint analysis with WL)

WFIRST strong point:
control of systematics

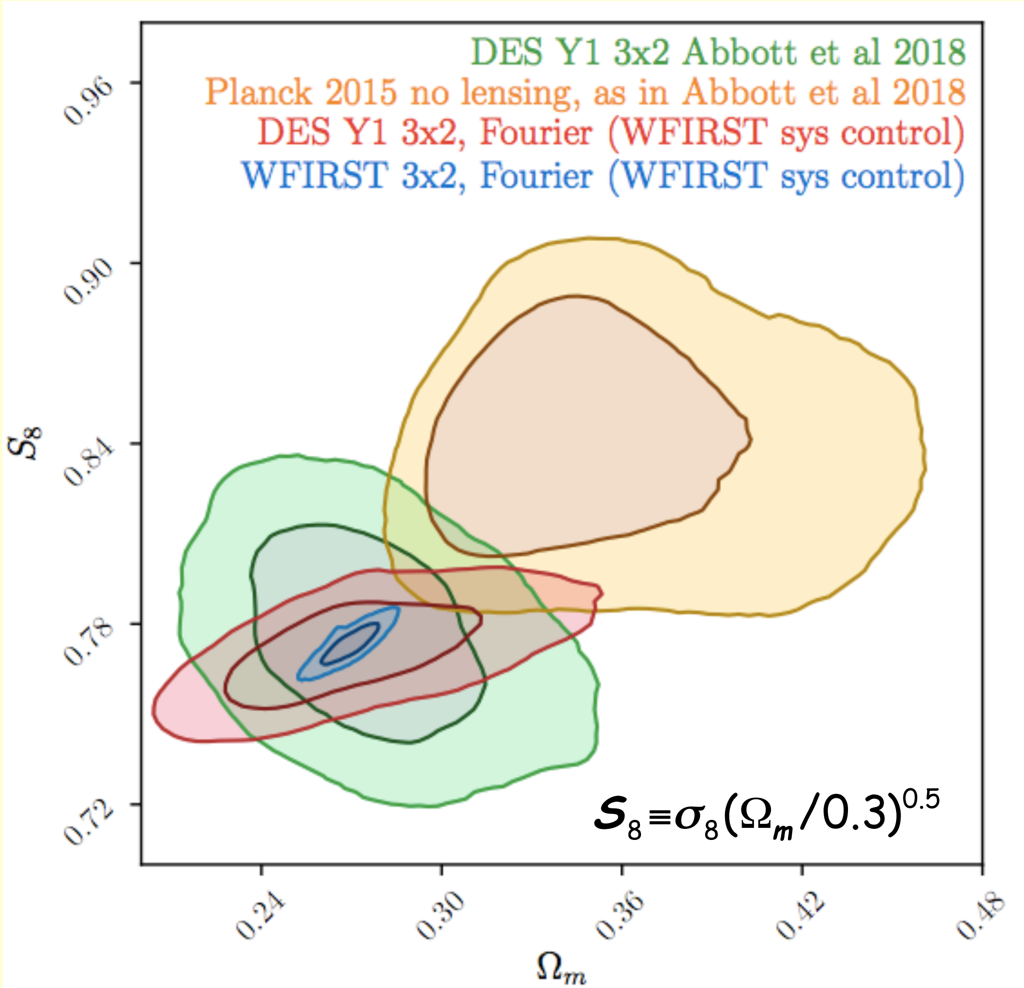

O. Doré et al, Astro2020 science white paper, arXiv:1904.011174

CONCLUSIONS

- weak lensing probes total matter distribution and imposes tight constraints on survey design & analysis to control systematics, esp. PSF control and calibration of source galaxy photo-z's.
- part of WL systematics can be self-calibrated via WL combination with clustering and galaxy-alaxy lensing.

- Prospects:
  - wide, dense, precise WL surveys are coming: Euclid, LSST, WFIRST
  - will all require external data to get reliable photo-z's:
    - multi-band imaging for photo-z determination
    - large sample of accurate spectra for photo-z algorithm training
    - large sample of accurate spectro-z's for photo-z error characterization

⇒ collaboration with existing/future ground-based surveys
collaboration between Euclid, LSST, WFIRST
proposals for new multi-object spectroscopy projects

Euclid, LSST, WFIRST

- Joint work: beneficial also for galaxy deblending, calibration of shear estimates, color-dependent PSF, residual shear systematics.... (& for other goals e.g. SNe, clusters, strong lensing ...)
- Similar statistical performance, different systematic uncertainty levels ⇒ combination

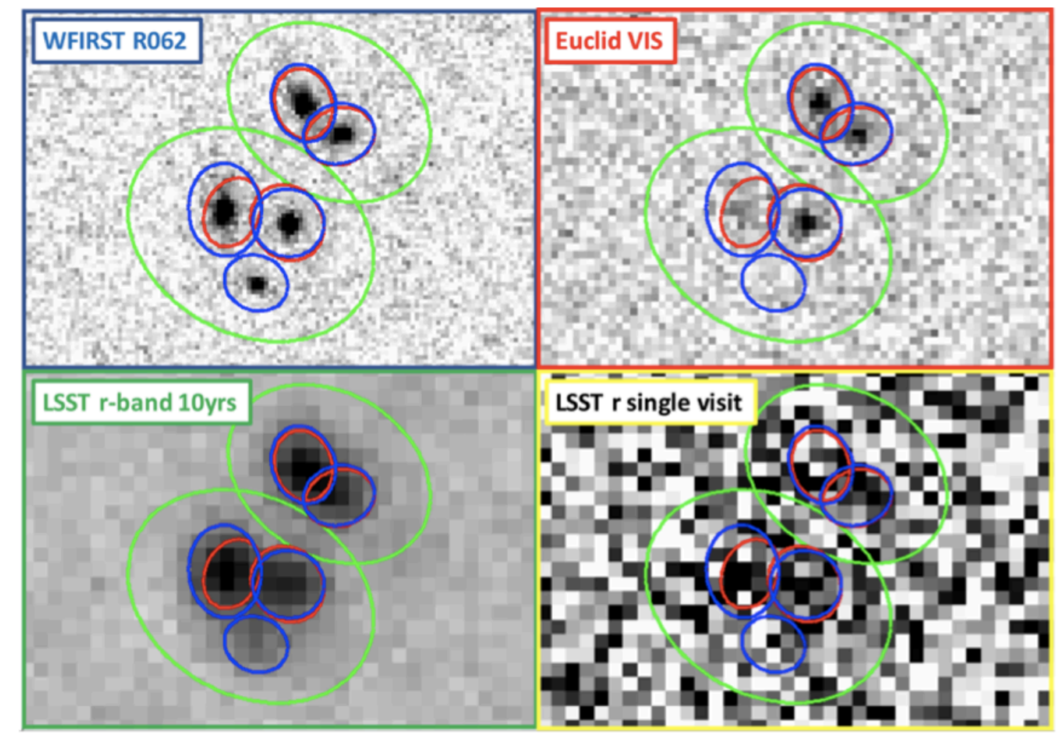

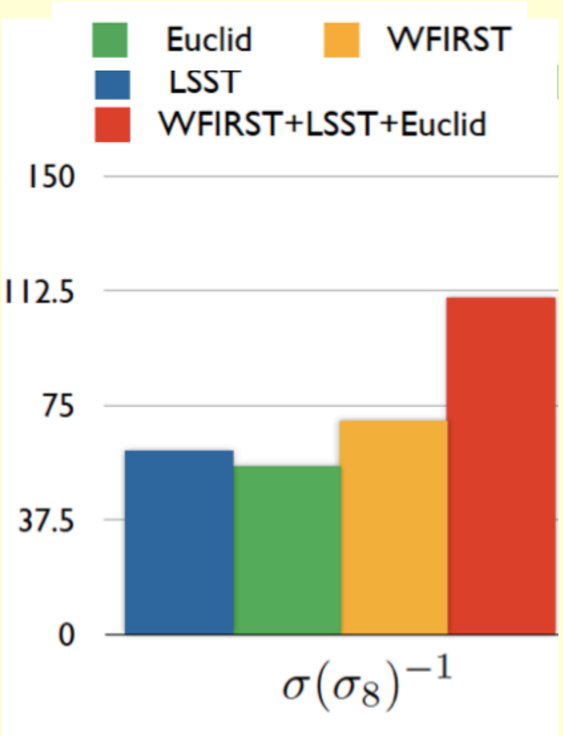

R.R.Chary et al, arXiv:1901.1259 *B.Jain et al, arXiv:1501.07897*

Back up slides

DES-Y1: one of the two shear measurements

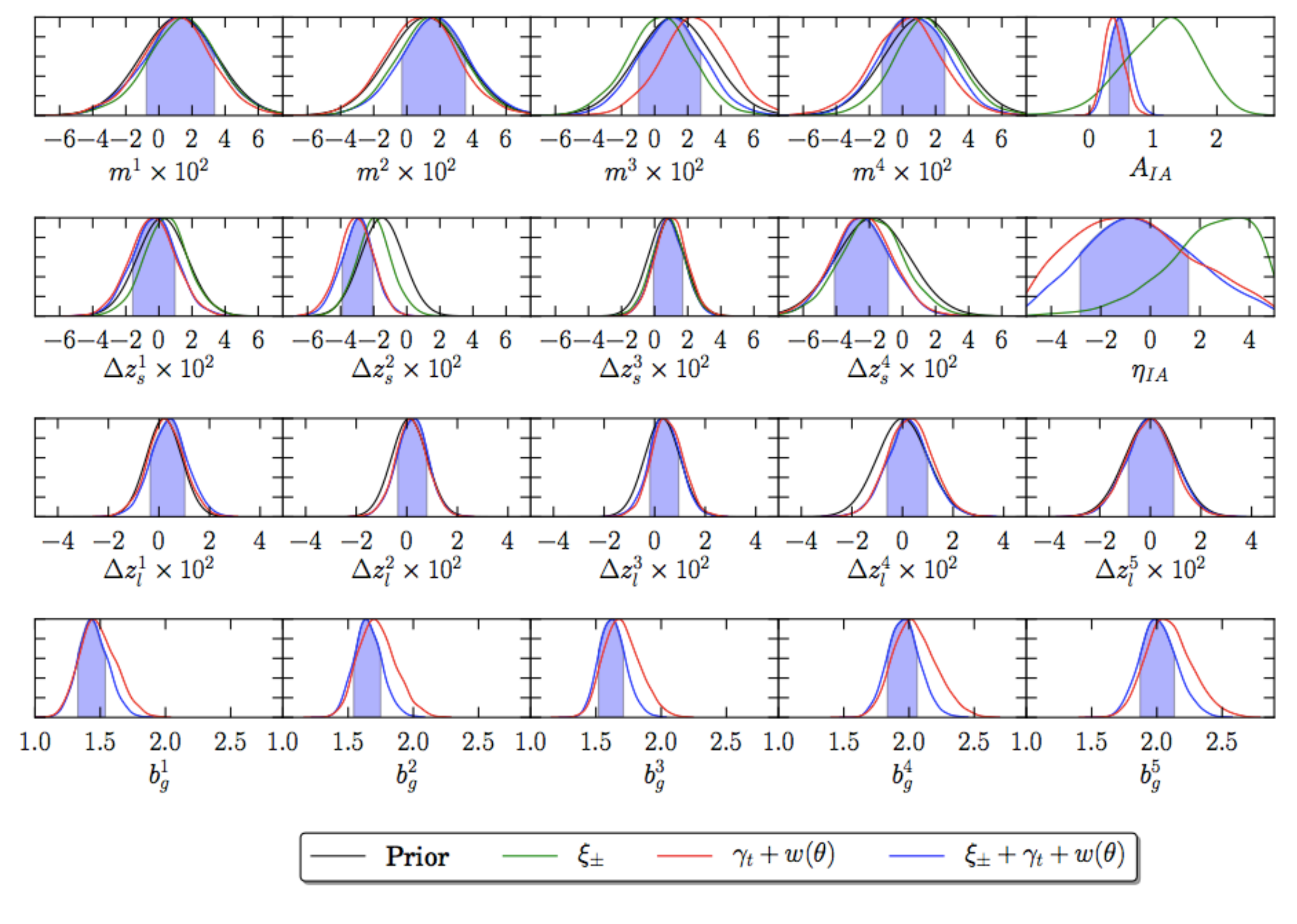

T.M.C.Abbott et al, 2018, Phys. Rev. D98, 043526

- Clustering data dominate intrinsic alignment parameter constraints and have a significant weight in the other constraints.

DES-Y1 joint analysis, impact of Σm_ν

- DES-Y1 analyses:
Σm_ν marginalized over

- Planck Λ_{CDM} analysis:
Σm_ν=0.06eV

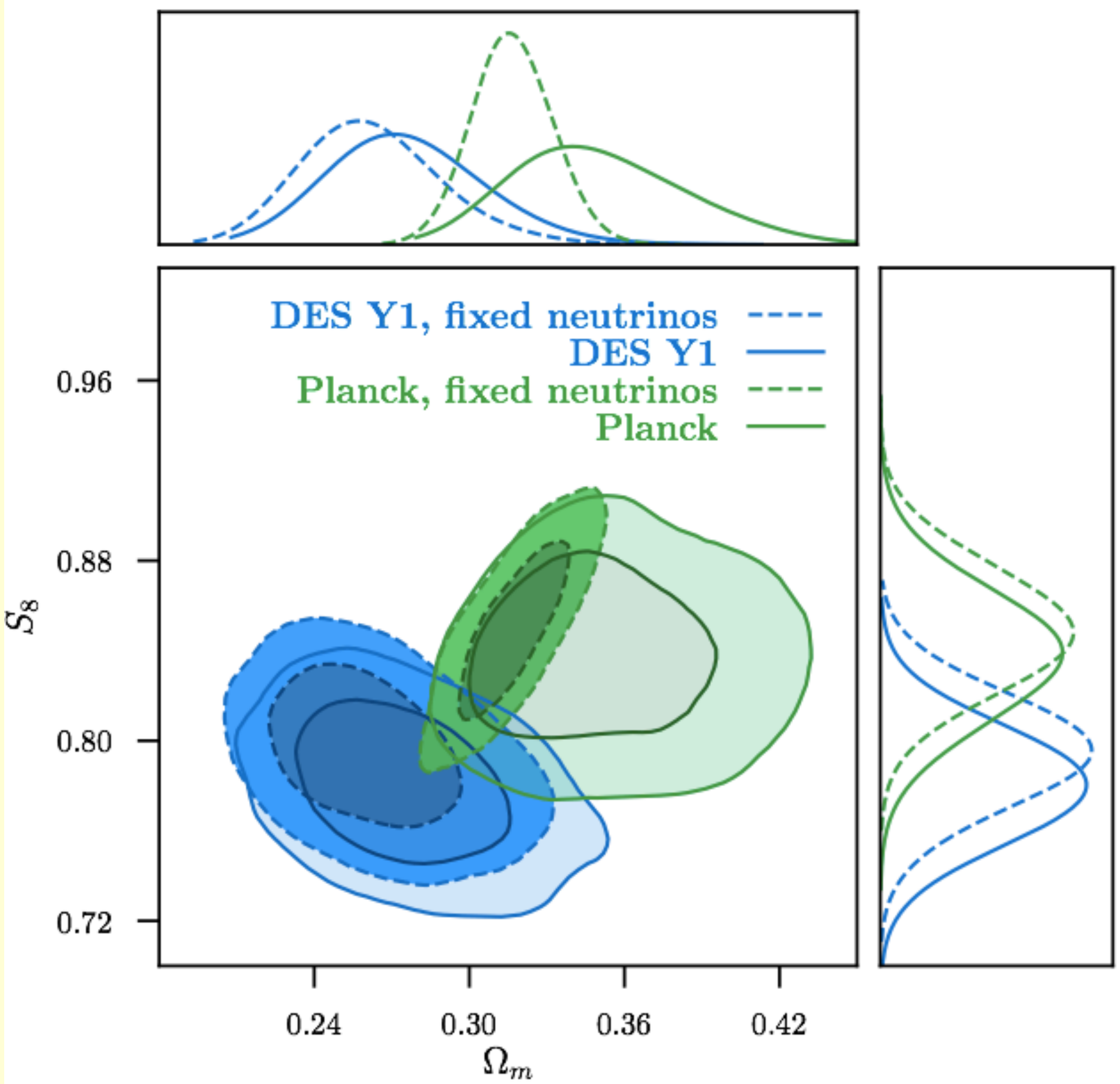

T.M.C.Abbott et al, 2018,Phys. Rev. D98, 043526

Planck-2018 vs DES Y1

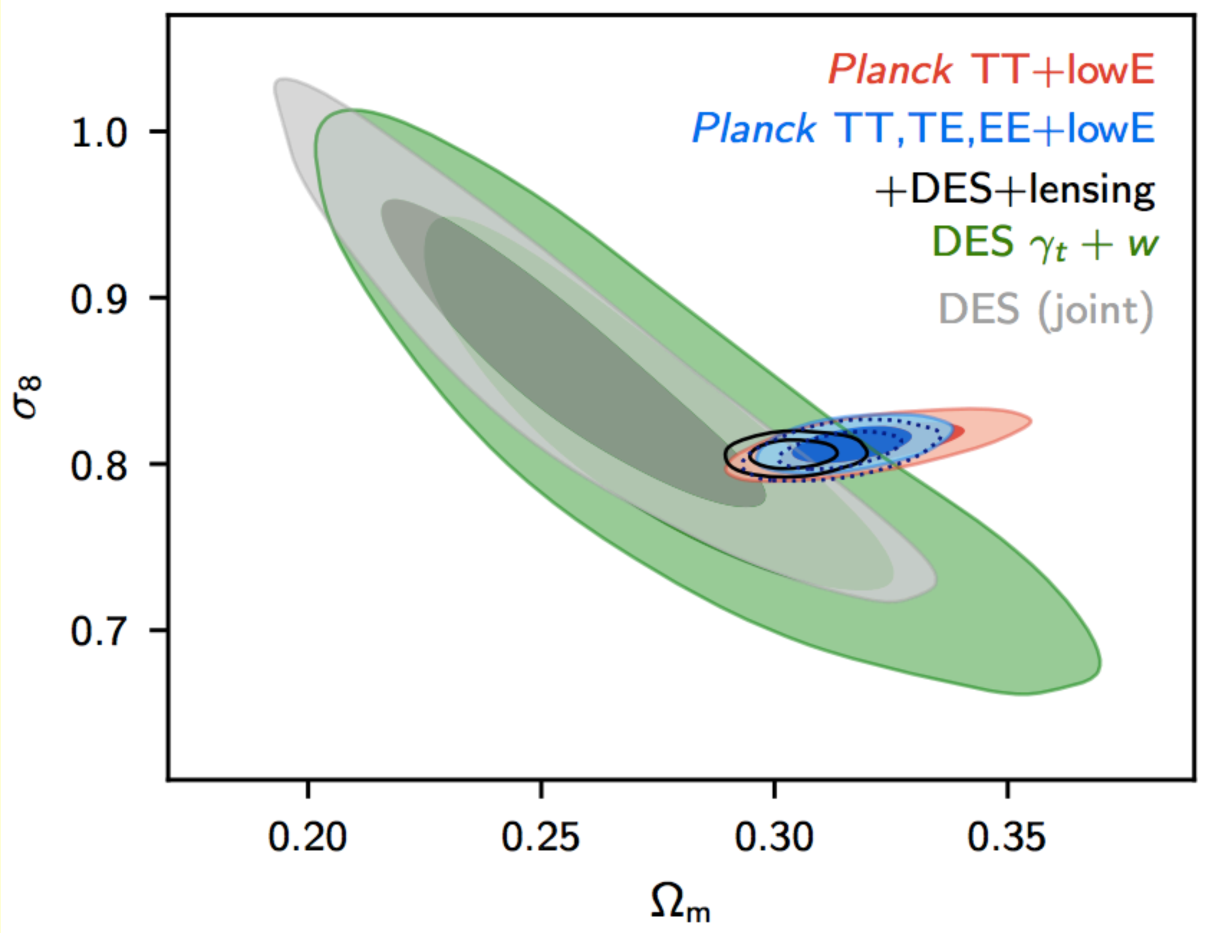

Planck Collab., arXiv:1807.06209

HSC-Y1

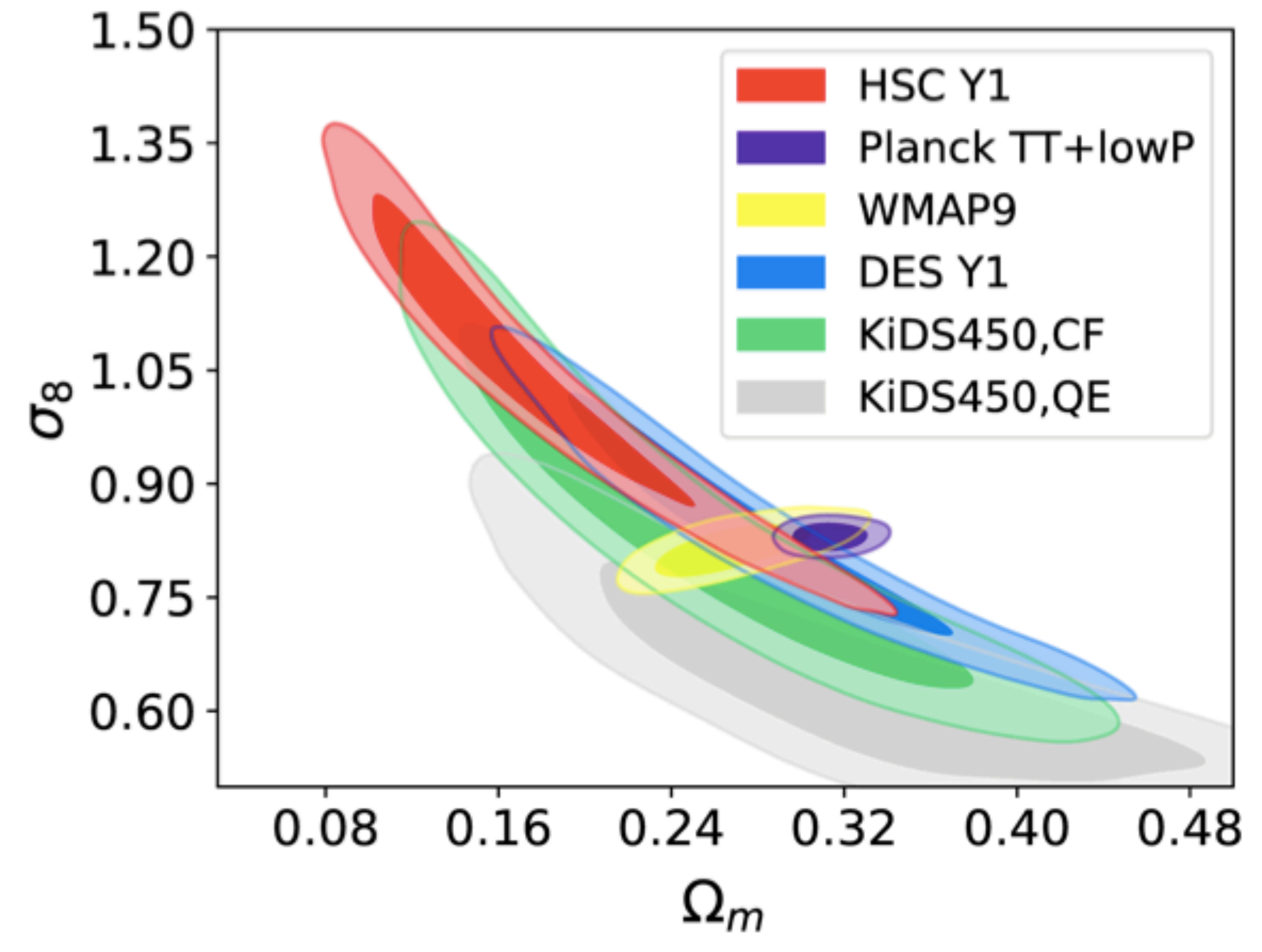

C.Hikage et al, 2019, PASJ,71, 43H

KiDS-VIKING-450

Table 1. Spectroscopic redshift surveys used for the calibration of KV450 photo-z.

Survey	Area [deg^2]	No. of spec-z	z-max	$r_{\rm lim}$	Used for
SDSS*	119.2	15564	0.7		CC/OQE
GAMA*	75.9	79756	0.4	19.8	CC/OQE
2dFLenS*	61.2	3914	0.8		CC/OQE
WiggleZ*	60.1	19968	1.1		CC/OQE
zCOSMOS	0.7	9930	1.0	24	CC/DIR
DEEP2	0.8	6919	1.5	24.5	CC/DIR
VVDS*	1.0	4688	1.3	25	CC/DIR
G15Deep*	1.0	1792	0.7	22	DIR
CDFS	0.1	2044	1.4	25	DIR

H.Hildebrandt et al, arXiv:1812.06076

- Enlarged sample of spectroscopic redshifts ⇒ reduced shot noise and sample variance in source photo-z calibration

KiDS-VIKING-450

Table 5. Setups for further MCMC test runs.

no.	Setup	Difference w.r.t. fiducial setup
1	sDIR	sDIR (smoothed version of DIR) $n(z)$
2	DIR-w/o-COSMOS	DIR $n(z)$ based on all spec-z except COSMOS
3	DIR-w/o-COSMOS&VVDS	DIR $n(z)$ based on all spec-z except COSMOS and VVDS
4	DIR-w/o-VVDS	DIR $n(z)$ based on all spec-z except VVDS
5	DIR-w/o-DEEP2	DIR $n(z)$ based on all spec-z except DEEP2
6	DIR-C15	DIR $n(z)$ based on the COSMOS-2015 photo-z
7	CC-fit	$n(z)$ from GMM fit to small-scale clustering-z (CC; App. C.2)
8	CC-shift	DIR $n(z)$ shifted to best fit CC measurements
9	OQE-shift	DIR $n(z)$ shifted to best fit large-scale clustering-z (OQE; App. C.3)
10	no-deltaz	redshift uncertainty switched off, i.e. $\delta z_i = 0$
11	IA-Gauss	informative Gaussian prior on $A_{\rm IA}$
12	IA-linear-PS	using the linear power spectrum in Eqs. 9
13	IA-z-evolution	allowing for redshift evolution in the IA model
14	no-baryons	baryon feedback switched off, i.e. $B = 3.13$
15	wide-baryons	wide prior on baryon feedback, $B \in [1.4, 4.8]$, $\eta_0 \in [0.4, 0.9]$
16	no-systematics	no marginalisation over nuisance parameters, no error on m
17	no-systematics_merr	same as 16 but including a $\sigma_m = 0.02$ uncertainty in the m-bias
18	all-xip	all scales $0\farcm5 < \theta < 300'$ used for ξ_+
19	nu0	massless neutrinos
20	nu0p26	one massive neutrino with $m = 0.26$ eV and two massless neutrinos
21	no-bin1	using tomographic bins 2, 3, 4, and 5 only
22	no-bin2	using tomographic bins 1, 3, 4, and 5 only
23	no-bin3	using tomographic bins 1, 2, 4, and 5 only
24	no-bin4	using tomographic bins 1, 2, 3, and 5 only
25	no-bin5	using tomographic bins 1, 2, 3, and 4 only
26	iterative-covariance	analytical covariance based on the best-fit fiducial cosmology

H.Hildebrandt et al, arXiv:1812.06076

Λ_{CDM} constraints on S_8 and Ω_m

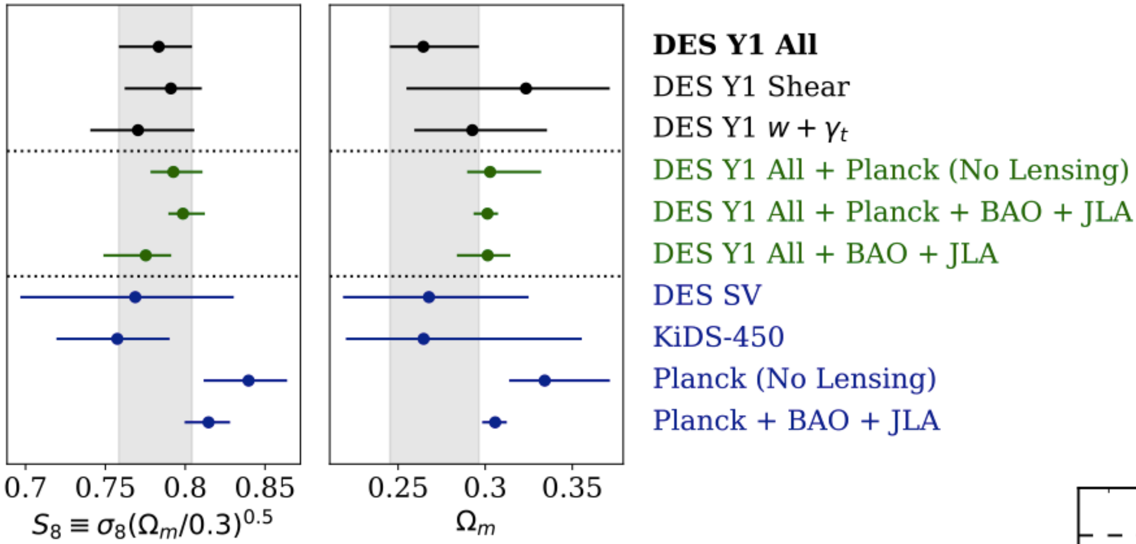

T.M.C.Abbott et al, 2018, Phys. Rev. D98, 043526

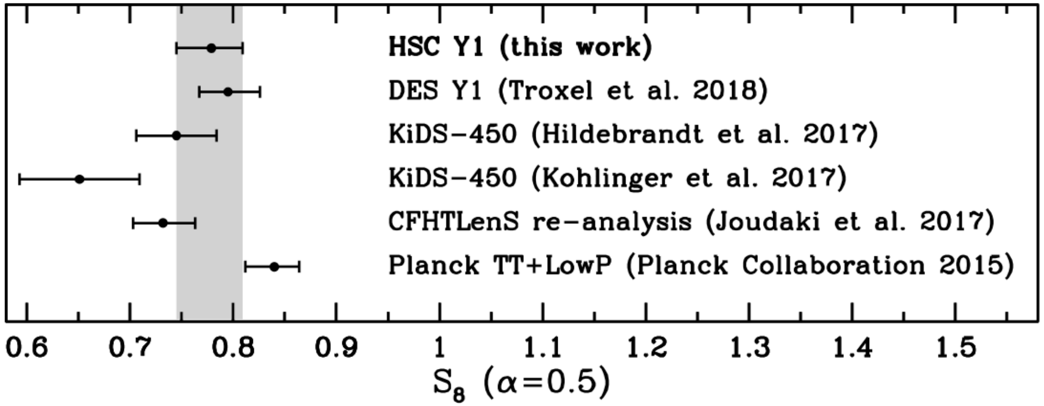

C.Hikage et al, 2019, PASJ,71, 43H

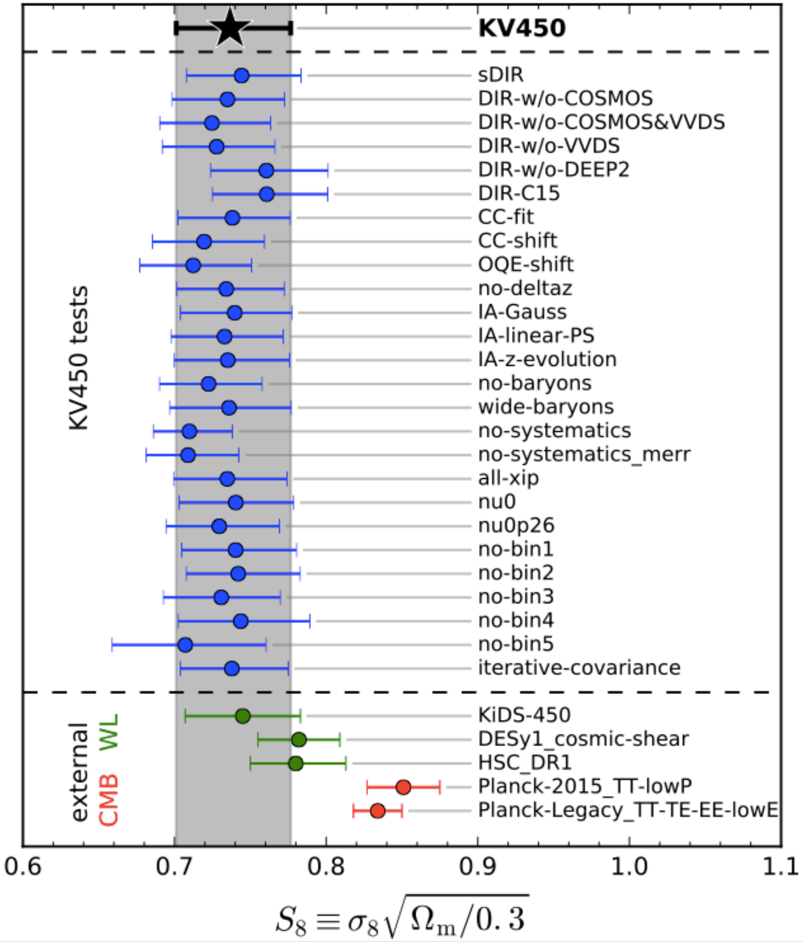

H.Hildebrandt et al, arXiv:1812.06076